Title

The Effects of Macrophage and Muscle Stem Cell-Specific Spp1 on Cell-Cell Interactions in Dystrophic Muscle



Author

Aragon, Raquel Linda

Publication Date

2023

Peer reviewed|Thesis/dissertation

UNIVERSITY OF CALIFORNIA

Los Angeles

# The Effects of Macrophage and Muscle Stem Cell-Specific Spp1 on Cell-Cell Interactions in Dystrophic Muscle

A dissertation submitted in partial satisfaction of the requirements for the degree Doctor of Philosophy in Molecular Biology

by

Raquel Linda Aragón

2023

ABSTRACT OF THE DISSERTATION

The Effects of Macrophage and Muscle Stem Cell-Specific Spp1 on Cell-Cell Interactions in Dystrophic Muscle

by

Raquel Linda Aragón

Doctor of Philosophy in Molecular Biology

University of California, Los Angeles, 2023

Professor Melissa J. Spencer, Chair

Duchenne muscular dystrophy (DMD) is one of the most common inherited, lethal childhood diseases. This X-linked recessive disorder is often caused by mutations in the *DMD* gene that leads to loss of functional dystrophin protein and results in myofibers that are susceptible to membrane rupture. Sarcolemmal fragility leads to chronic cycles of muscle degeneration and regeneration and a subsequent reprogramming of the muscle niche that includes unresolved inflammation, defective muscle stem cell activity, aberrant pathological fibrosis, intramuscular adipose tissue (IMAT) accumulation and ultimately failed regeneration. Our lab has shown that osteopontin (SPP1) is a critical regulator of DMD disease progression that links many of these processes through its complex biology. SPP1 is multifunctional matricelluar protein, encoded by the *Spp1* gene, that is post-translationally modified in many ways, expressed by a host of different cells in the muscle niche and can bind to a plethora of different receptors. This complexity can greatly impact how SPP1 acts on target cells and the

signaling cascades that result in DMD disease progression. In this dissertation, we utilized single cell RNA sequencing to unbiasedly explore how two cell-specific sources of SPP1, macrophage-derived and muscle stem cell-derived, affect cell-cell interactions in dystrophic muscle.

Here we show that macrophage-derived SPP1 is an autocrine regulator of macrophage TGFβ1. We identified two novel adipogenically primed stromal cell populations that are regulated by macrophage-derived TGFβ and contribute to IMAT. Our work established a link between macrophage-derived SPP1, reduced macrophage-derived TGFβ and ectopic fatty infiltration that is a hallmark of progressive DMD. Additionally, we showed that muscle stem cell (MuSC)-specific SPP1 has an autocrine inhibitory effect on MuSC stemness and positive effect on the fibrotic and inflammatory phenotype of MuSCs. Endothelial cells greatly expand in the MuSC Spp1 cKO showing a pro-angiogenic, anti-inflammatory state. We hypothesize that MuSC-derived SPP1 crosstalks with endothelial cells (ECs), leading to reduced EC expansion and an anti-angiogenic, pro-inflammatory, activated state. Furthermore, we provide evidence that this MuSC-EC regulatory axis affects macrophage phenotype. Altogether, this work advances knowledge of cell-specific SPP1 biology that drives DMD disease progression.

The dissertation of Raquel Linda Aragón is approved.

Hilary Ann Coller

Rachelle Hope Crosbie

Brigitte N. Gomperts

Melissa J. Spencer, Committee Chair

University of California, Los Angeles

2023

# DEDICATION

*Para mi Tita, Cirenia Aragón Solis, en el cielo y en mi corazón. Gracias por su sacrifício por el futuro de nuestra familia. Mis éxitos son sus éxitos.*

*And to my ancestors who passed down their resilience from generation to generation. Thank you for blessing my spirit with your strength to push through the difficult times.*

Table of Contents

LIST OF FIGURES

# ACKNOWLEDGEMENTS

I am completing this dissertation because of the village of people who believed in me and armed me with the strength to keep going. First, I am forever indebted to my advisor, Dr. Melissa Spencer, who gave me a second chance at fulfilling this life goal. My gratitude for your relentless belief in me, your hard-fought patience, and unwavering encouragement cannot be fully expressed in words. Your mentorship was healing throughout a very rocky graduate school experience. Thank you for keeping your word in helping me get through the finish line.

I want to thank all the members of the Spencer lab for welcoming me into your community and helping these projects become what they are. To Dr. Irina Kramerova, you were a constant source of knowledge and support. Thank you for your patience and for teaching me everything you could. Dr. Michael Emami, you're the reason I got a second chance. Robert Jimenez, thank you for bringing joy to many tough days with dinosaur stickers and our heart-to-hearts. And to Justin Amakor and Bradley Smith, thank you for allowing me to teach you and for being my right and left hands – I could not have done this without you. Additionally, I would like to thank Dr. Chino Cresse for laying such a strong foundation for these projects.

Next, I am grateful for my thesis committee: Dr. Hilary Coller, Dr. Brigitte Gomperts and Dr. Rachelle Crosbie for your professional and personal support. Special thanks to Dr. Rachelle Crosbie, alongside Dr. Melissa Spencer, for creating a supportive muscle biology trainee group. This community was profoundly important for my growth as a muscle biologist.

I would also like to thank Dr. Luisa Iruela-Arispe for being my first advisor in graduate school. I am so grateful that I got to learn from you. Thank you for setting me up for success. Special thanks to all the Arispe lab members I got to work with for your support and wisdom. I, especially, want to acknowledge Dr. Gloria Hernandez who became my family. Your friendship is one of the best things that I was given during grad school.

I was lucky to find a strong community outside of my research that played a big role in my professional and personal development. Thank you to the members of the Association for Multi-Ethnic Bioscientists' Advancement for teaching me how to become an advocate and a leader and for becoming my village. I am eternally grateful for the friends and colleagues in the Center for Education Innovation and Learning in the Sciences, especially Dr. Katie Dixie, for giving me the tools and encouragement to reach my lifelong goal of being a science educator.

Finally, I would not have reached this milestone without the lifelong love and support from my family. To my dad Jerry Witt, thank you for being the father I needed and deserved. I am lucky to have sisters, Ari Witt and Taylor Witt, who are beautiful examples of what happens when you work hard. To my partner, Ricardo Azevedo, thank you for holding my hand through every up and down and reminding me that it would all be worth it. And thank you to my mom, Ruth Aragón Witt, who sacrificed more than one person should to make our lives the best they could be. This is all for you.

# VITA

## EDUCATION

Bachelor of Arts, Biochemistry, *cum laude* 2010 – 2014
*Mount Holyoke College*, South Hadley, MA

---

## RESEARCH EXPERIENCE

- **PhD Candidate** 2019 – present

Advisor: Dr. Melissa Spencer, *University of California, Los Angeles*

- **Graduate Student Researcher/PhD Candidate** 2016 – 2019

Advisor: Dr. Luisa Iruela-Arispe, *University of California, Los Angeles*

- **Research Assistant** 2014 – 2016

Advisor: Dr. Charles Gilbert, *The Rockefeller University*

- **Undergraduate Student Researcher** 2010 – 2014

Advisor: Dr. Megan Nuñez, *Mount Holyoke College*

- **Summer Undergraduate Research Fellow** Summer 2013

Advisor: Dr. Mary E. Hatten, Summer Undergraduate Research Fellowship
*The Rockefeller University*

- **Amgen Scholar** Summer 2012

Advisor: Dr. Michael McManus, Amgen Scholar Program
*University of California, San Francisco*

---

## TEACHING EXPERIENCE

- **Research Mentor**, *UCLA*

Justin Amakor (Undergraduate Researcher) June 2022 – present
Bradley Smith (Work Study Student) September 2022 – present
Liliana Tinoco (Undergraduate Researcher) 2018 to 2019

- **Teaching Assistant**, *UCLA* Fall/Winter 2018, Fall 2022

Courses:
-Molecular, Cellular and Developmental Biology (MCDB) 165A, Biology of the Cell
-Biomedical Research (BMD RES) 5HB: Essential Skills and Concepts

- **Teaching Internship with Experienced Support (TIES) Program** Spring 2021

Faculty Mentor: Dr. Nikki Plaster, *Golden West College*
*Coast Community College District*

- **Co-Outreach Coordinator** 2017 – 2018

Society for the Advancement of Chicanos/Hispanics and Native Americans in Science (SACNAS), *UCLA*

- **Science Outreach Volunteer** 2015 – 2016

Science Saturday, *The Rockefeller University*

- **Peer Learning Undergraduate Mentor** 2011 – 2014

Courses: General Chemistry, Cell Biology, *Mount Holyoke College*

---

## HONORS AND AWARDS

- CIRTL@UCLA Scholar Certification May 2023
- CIRTL@UCLA Travel Award December 2022
- UCLA Muscle Cell Biology, Pathophysioloy, and Therapeutics Training Grant June 2022
- UCLA MBIDP Eiserling/Lengyel Teaching Excellence Award September 2021
- UCLA MBIDP Outstanding Poster Award September 2021

- UCLA MBIDP Diversity, Equity and Inclusion Award September 2020
- UCLA Taylor M. Brown Memorial Award September 2020
- Best Elevator Pitch,UCLA Center for Duchenne Muscular Dystrophy Retreat February 2020
- SACNAS Travel Award, *Deferred* June 2019
- HHMI Gilliam Graduate Fellowship June 2018
- National Science Foundation GRFP, *Honorable Mention* April 2018

---

**LEADERSHIP**

**Graduate Student Representative** Fall 2021 – Spring 2022
Life Sciences Diversity Advisory Committee, *UCLA*

- **Chief Financial Officer** Summer 2018 – Spring 2022

Association of Multi-Ethnic Bioscientists' Advancement, *UCLA*

- **Co-Chair** Fall 2018 – Summer 2021

Scientific Excellence through Diversity Seminar Series, *UCLA*

- **Co-Chair** Summer 2017, 2018

Women in STEM panel, Equity, Diversity and Inclusion Day, *UCLA*

---

**PEER-REVIEWED PUBLICATIONS**

- McDonald, A.I., Shirali, A.S., **Aragón, R**., Ma, F., Hernandez, G., Vaughn, D.A., Mack, J.J., Lim, T., Sunshine, H., Zhao, P., Kalinichenko, V., Hai, T., Pelegrini, M., Ardehali, R., Iruela-Arispe, M.L. Endothelial regeneration of large vessels is a biphasic process driven by local cells with distinctproliferative capacities. 2018. Cell Stem Cell.
- Mack, J.J., Mosquiero, T.S., Archer, B.J., Jones, W.M., Sunshine, H., Faas, G.C., Briot, A., **Aragón,R.L**., Su, T., Romay, M.C., McDonald, A.I., Kuo, C.H., Lizama, C.O., Lane, T.F., Zovein, A.C., Fang,Y., Tarling, E.L., de Aguilar, Vallim, T.Q., Navab, M., Fogelman, A.M., Bouchard, L.S., Iruela-Arispe, M.L., NOTCH1 is a mechanosensor in adult arteries. 2017. Nature Communications 8(1), 1620.

# Chapter 1 – Introduction

## *Duchenne muscular dystrophy*

Duchenne muscular dystrophy (DMD) is one of the most common deadly childhood genetic diseases with an incidence rate of 1 in 3800 – 6200 male births[1]. This X-linked recessive disorder presents in boys early in childhood as severe and progressive muscle degeneration. Chronic muscle degeneration in DMD patients leads to loss of ambulation in early adolescence, and ultimately, premature death around age 25. DMD is caused by mutations in the *DMD* gene, encoding for dystrophin protein, leading to loss of functional protein expression at the muscle cell membrane (sarcolemma)[2]. In normal muscle tissue, dystrophin is critical for maintaining sarcolemmal integrity as the N-terminus binds to the actin cytoskeleton and a C-terminal domain binds to the dystrophin glycoprotein complex (DGC)a sarcolemmal protein complex, that allows the cell to interact with the extracellular matrix[3]. In addition, dystrophin protein has a central rod region containing spectrin-like repeats that act as molecular shock absorbers that protect muscle fibers from normal contraction/relaxation and acute injury[1,3]. Lack of functional dystrophin expression makes the sarcolemma susceptible to contraction-induced injury leading to chronic cycles of muscle degeneration and regeneration[4]. DMD patient muscles lose muscle stem cells (MuSCs) with time due to chronic cycles of degeneration and regeneration. Eventually regenerative capacity fails due to the inflammatory environment and the constant drive for MuSC activation[5,6]. Loss of dystrophin also affects the asymmetric division of MuSCs, needed for replenishment of MuSCs in the niche[7].

## *Existing therapeutic strategies for DMD*

There is currently no cure for DMD. The gold standard of care for patients is treatment with glucocorticosteroids, like prednisone and deflazacort, which have been shown to improve muscle strength and pulmonary function and delay loss of ambulation and onset of cardiomyopathies[8]. Glucocorticosteroids likely reduce the aberrant inflammatory response

associated with DMD pathology[9]. Prednisone, specifically, has been shown to reduce a variety of immune cells such as macrophages, T-cells, and eosinophils in *mdx* muscle and reduces vascular adhesion molecules that aid in immune infiltration[10]. Additionally, studies have shown that glucocorticosteroids have a direct impact on muscle fiber gene expression of annexins, which have dual roles in promoting sarcolemmal repair and regulating immune response resolution[11]. However, long-term steroid treatment is associated with adverse effects such as weight gain and changes in behavior[12].

Emerging therapeutic approaches are focused on fixing the primary cause of DMD – restoring dystrophin expression in skeletal muscle via gene therapy strategies. Mostly recently, the first gene therapy for DMD was approved by the FDA in June 2023[13]. This AAV-based gene therapy commonly known as ELEVIDYS delivers a truncated, but still partially functional, 138kDA version of dystrophin protein, called micro-dystrophin, and has been approved for patients ages 4-5 years old who are still ambulatory[13]. While this is a turning point in the treatment of DMD patients, gene therapy approaches still have significant adverse effects such as liver injury and thrombocytopenia[14].

*Osteopontin/SPP1 structure and function*

Osteopontin (SPP1) is a matricellular phosphoglycoprotein with cytokine-like properties. As its many alternative names imply such as bone sialoprotein 1 (BSP1), early T-lymphocyte activation 1 (ETA1) and secreted phosphoprotein (SPP1), osteopontin is known to affect a variety of biological processes[15]. Notably it was first isolated from bovine bone and is classically known for its role in bone morphogenesis[16]. However, is now known to be expressed in many cells types such as immune cells like macrophages, B-cells, and T-cells, vascular cells like endothelial cells and smooth muscle cells, as well as skeletal muscle, stromal cells and beyond[17–19].

The human form of SPP1 is made up of ~314 amino acids while the murine ortholog is made up of 297 amino acids[20]. SPP1 has a molecular weight ranging from 32 to 75kDa due to a

variety of post-translational modifications along its seven exons[15,17,20,21] (Figure 1.1). It has many functional domains that facilitate binding to a variety of receptor targets. These receptor targets include a range of integrins which can bind to the C-terminal RGD domain, the domain in humans[21]. Additionally, SPP1 can bind to other extracellular matrix molecules such as the glycosaminoglycan heparin, fibronectin, and collagen type I[21]. While SPP1 does not directly contribute to the structural integrity of the ECM, its ability to bind to many ECM molecules allows it to indirectly facilitate and alter important ECM component interactions. Most interestingly, SPP1 can bind CD44, a receptor known for binding hyaluronic acid and playing a role in lymphocyte/macrophage activation and migration[22].

These various binding domains contain sites of potential posttranslational modifications, many of which impact interactions between SPP1 and its binding partners and are cell-type specific. SPP1 contains over three-dozen serine, threonine and tyrosine residues that can be phosphorylated[15]. In addition, SPP1 contains sites of glycosylation, sulfonation, transglutamination and can be cleaved by proteases such as thrombin and matrix metalloproteases including MMP3, MMP7 and MMP9[15]. Cleavage by thrombin and MMPs is known to alter the adhesive properties of SPP1 to integrins by SVVYGLR domains[21].

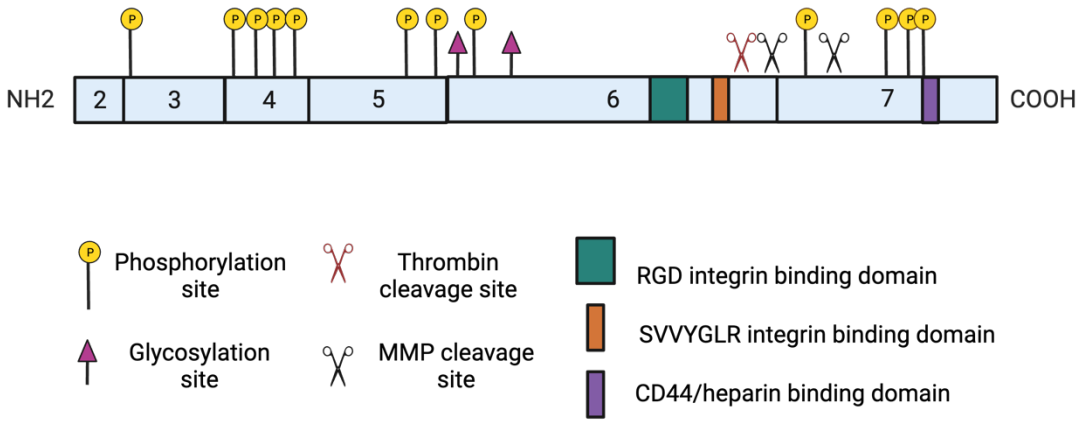


**Figure 1.1 Schematic of osteopontin protein structure and post-translational modification sites.** The six translated exons of osteopontin are numbered. Integrin binding sites (shown in

green and orange) and CD44/heparin binding sites (shown in purple) are shown in exons six and seven, respectively. Select post-translational modifications are shown such as predicted phosphorylation sites (yellow circles) and glyocosylation sites (purple triangles) are distributed throughout the protein. Additionally, cleavage sites for thrombin and MMPs reside in the C-terminal region (red and black scissors).

*Osteopontin in disease*

Due to its expression across a broad spectrum of cell types, the number of diverse ligand-receptor interactions and variety of potential posttranslational modifications, it is not surprising that SPP1 is known to play a role in many pathologies. It is highly upregulated in a range of inflammatory and autoimmune diseases such as multiple sclerosis[23,24], Crohn's disease[25], and rheumatoid arthritis. In multiple sclerosis, T cells expressing $\boldsymbol{\alpha_4\beta_1}$ bind to endothelial cells expressing osteopontin (and VCAM1) on the plasma membrane which allows the T cells to infiltrate the brain[24] – a process that is critically important in regulating relapse-remission of the disease. Concurrently, SPP1 is secreted by microglia, neurons, T cells and antigen-presenting cells which promote the survival of autoreactive T-cells via the inhibition of FOXO3A and the eventual damage of myelin-producing oligodricytes[23,24]. In Crohn's disease and rheumatoid arthritis, SPP1 was found to be highly expressed in IgG(+) plasma cells/a subset of macrophages in human inflamed intestinal mucosa and CD4(+) T cells in synovial fluid/joints/lining, respectively[26,27].

SPP1 also plays a role in cardiovascular diseases like acute and chronic ischemia[28], atherosclerosis[29], and hypertension[30], all of which involve leukocytes in disease progression. In a mouse model of accelerated atherosclerosis, ablation of SPP1 led to a striking reduction in atherosclerotic lesions and reduction of lipid laden macrophages within fatty streaks of the vessel wall[31]. Interestingly, they found that SPP1-derived from the bone marrow, was an important driver of atherosclerotic lesions in the aorta[31]. These studies suggest that SPP1 is a critical regulator of proper innate and adaptive immune responses.

*Osteopontin in Duchenne muscular dystrophy*

SPP1 is highly expressed in muscle biopsies of DMD patients[32]. In 2011, a study of two cohorts of DMD patients identified *Spp1* as a genetic modifier of DMD disease severity[33]. The study found a G minor allele (TG/GG) in SNP rs28357094, located upstream of the *Spp1* transcriptional start site, was associated with patients with significantly reduced grip strength and earlier loss of ambulation compared to patients with the more common T allele[33]. Interestingly, while some studies have shown that polymorphisms in the *Spp1* promoter region may mitigate its transcriptional activity, this same group found that the DMD patient biopsies with minor alleles (TG/GG) at rs28357094 were not associated with higher SPP1 mRNA or protein expression compared to DMD patients with the TT allele[32].

Our lab previously found that global ablation of SPP1 in the *mdx* mouse model of DMD mitigated disease severity[18,34]. SPP1$^{-/-}$ mdx mice showed an overall improved muscle phenotype including increased muscle regeneration, improved muscle function, reduced fibrosis, and a shift towards a pro-regenerative immune response[18,34]. Notably, ablation of SPP1 led to a significant reduction in *Tgfb1* expression, which encodes for TGF**β**1, a pro-fibrotic cytokine that is also upregulated in DMD[18,19] and is associated with pathological fibrosis. This suggests that *Spp1* is a modifier of *Tgfb*.

*TGF**β** and LTBP4 in Duchenne muscular dystrophy*

TGF**β** proteins are regulated by latent TGF**β** binding proteins (LTBPs). LTBP4, specifically, is a chaperon that aids TGF**β** protein folding and secretion. Additionally, LTBP4 plays a critical role in regulating TGF**β** activation as it sequesters the cytokine in its latent form within the ECM[35]. Proteolytic cleavage of LTBP4 allows the release of the active form of TGF**β**[35], which can then subsequently go on to bind to its cognate TGF**β** receptors on different cell types and activate downstream signaling molecules such as pSMAD2/3. *Ltbp4* is a known modifier of muscular dystrophy in mice[36] and humans[37]. In a large DMD patient cohort, a risk *Ltbp4* haplotype was found to be correlated with earlier loss of ambulation[37]. Fibroblasts

genotyped to have the risk alleles showed higher pSMAD2/3 activation compared to fibroblasts with the protective *Ltbp4* alleles when treated with latent TGF**β** suggesting a reduced capacity to sequester TGF**β**[37].

*Significance*

The work in this thesis aims to lay the framework for understanding SPP1's mechanism of action in dystrophic muscle in a cell specific manner. Considering that SPP1 is one of the most highly expressed proteins in DMD understanding the impact of different cellular sources of SPP1 is important for elucidating cell-cell communication pathways that affect disease progression. SPP1 is primarily considered an immune regulator, but this thesis uses single cell RNAseq as an unbiased approach to undercover direct and indirect cell-specific effects of SPP1 on other cell types in the muscle niche such as stromal cells, MuSCs, and endothelial cells that play critical roles in fibrosis, fat infiltration and muscle regeneration. This thesis provides foundational knowledge for assessing on-target activity of possible SPP1 inhibitors that would benefit DMD as well as other disease in which SPP1 plays a critical role.

# Chapter 2 – Effect of macrophage-derived Spp1 on the dystrophic muscle niche


## ABSTRACT

Duchenne muscular dystrophy (DMD) is a genetically inherited, progressive muscle wasting disorder caused by mutations in the *DMD* gene, which encodes for dystrophin protein. In DMD, chronic cycles of degeneration and regeneration lead to aberrant inflammation and accumulation of fibrosis and fat in skeletal muscle. Our previous work showed that osteopontin (Spp1) is a critical regulator of DMD disease progression[18,34]. Global knockout of *Spp1* in dystrophic mice (Spp1 KO) led to and an overall improvement in muscle regeneration, reduced fibrosis and enhanced muscle function. Correlated with these changes were a shift in macrophage polarization towards M2c, which is considered a pro-regenerative macrophage phenotype. Spp1 is expressed by a variety of cells within the muscle niche and can be post-translationally modified in many ways that could impact its binding to local receptors, leading to differential effects on target cells. How cell-specific sources of Spp1 influence cellular dynamics in dystrophic muscle is currently not known. In this study we used single cell transcriptomics to uncover how macrophage derived Spp1 impacts cell-cell interactions in *mdx* muscles. We found that ablation of macrophage-specific *Spp1* (Mϕ cKO) had an autocrine effect on macrophage polarization away from an M1-like phenotype and a reduction in *TGFβ1* expression in M2-like macrophages. Additionally, we identified two novel stromal cell populations that are enriched in adipogenesis genes. These stromal cells are greatly reduced in the absence of macrophage derived Spp1, and this reduction correlated with reduced intramuscular fat in diaphragms. Our data reveals a role for macrophage derived Spp1 as a regulator of TGFb1 and maintenance of a novel stromal cell population that contributes to intramuscular fat deposition.

INTRODUCTION

Duchenne muscular dystrophy (DMD) is one of the most common inherited, deadly childhood diseases[1]. This X-linked recessive disorder is caused by mutations in the *DMD* gene that encodes for the dystrophin protein, an important sarcolemmal membrane that protects myofibers from contraction and injury-induced mechanical stress[2]. Lack of functional dystrophin expression causes sarcolemmal fragility leading to chronic cycles of muscle degeneration and regeneration.

In an acute injury setting, healthy muscle follows a carefully orchestrated muscle regeneration and repair process that is initiated by infiltration of neutrophils and Ly6c$^{hi}$, F4/80$^{lo}$ monocytes to the damaged area[34,38]. These monocytes go on to differentiate from a pro-inflammatory phenotype towards a pro-regenerative Ly6c$^{lo}$, F4/80$^{hi}$ macrophage phenotype[34,38]. This phenotypic switch is necessary for acute activation and expansion of stromal cells, including fibro-adipogenic progenitor (FAPs) cells and fibroblasts, that lay down the connective tissue that provides structural support for the damaged site[39]. The microenvironment established by this precisely regulated inflammatory and stromal cell response allows for activation of muscle stem cells (MuSC) that go on to fuse, differentiate and regenerate myofibers[40,41].

In chronic injury settings, such as in DMD, a dysregulated inflammatory response occurs in which there is a prolonged presence of both pro-inflammatory and anti-inflammatory macrophages leading to the accumulation of the pro-fibrotic cytokine, TGFβ[42]. Subsequently, there is an aberrant and unresolved stromal cell expansion that results in chronic fibrosis, failed myogenesis and a subsequent intramuscular adipose tissue (IMAT) infiltration[43].

We previously identified osteopontin (Spp1) as a modifier of TGFβ1 expression in *mdx* muscle. The *Spp1* gene encodes for osteoponin, a matricellular protein that is highly upregulated in dystrophic muscle[18,19,34]. Global knockout of *Spp1* in *mdx* mice showed an improved dystrophic phenotype including increased muscle function, increased muscle fiber

regeneration, increased polarization towards pro-regenerative macrophages, reduced *TGFβ1* expression, and reduced collagen deposition suggesting reduced fibrosis compared to *mdx* mice[18,19,34].

SPP1 is a highly complex protein involved in a diverse array of biological processes and signaling pathways. SPP1 can be secreted or reside intracellularly. In the extracellular matrix, it can bind to a variety of receptors and other proteins such as integrins, CD44, and heparin[21]. SPP1 is expressed by a variety of cell types within the skeletal muscle niche such as immune cells, stromal cells, muscle fibers, endothelial cells and muscle stem cells[15,18,19,21,34]. Additionally, SPP1 can be post-translationally modified by phosphorylation, glycosylation, transglutamination, and cleaved by thrombin and metalloproteases. In addition, depending on the source of SPP1, the post-translational modifications and the effects on target cells may differ[15]. How cell specific sources of SPP1 impact different target cells in the highly dynamic dystrophic niche is not understood.

Here we use single cell RNA sequencing to elucidate how macrophage-derived SPP1 impacts the cellular milleu of the dystrophic skeletal muscle niche. We show that conditional ablation of myeloid-specific *Spp1* in mice on the *mdx* background (Mϕ cKO) has a significant paracrine effect on the heterogeneity of stromal cell populations, leading to the disappearance of two previously uncharacterized adipogenically primed stromal cell subtypes. Additionally, Mϕ cKO mice show a shift towards M2-like macrophages that have reduced *TGFβ1* expression, suggesting that *TGFβ1* is necessary to maintain these populations. By using single cell sequencing, this study provides insight on how macrophage-specific SPP1 regulates and promotes a fibro-inflammatory immune response and a pro-adipogenic microenvironment in dystrophic muscle.

## MATERIALS AND METHODS

### *Animal husbandry*

Guidelines from the Animal Research Committee at UCLA were followed in the handling and breeding of all mice. Protocols for the care and use of animals were approved by the UCLA Office of Protection of Research Subjects.

*Generation of Spp1 conditional knockout targeting vector*

The Spp1 region of accession #NT_109320.5 (28,332,597-28,344,133) was cloned into pBlueScript II SK(+) and inserted into the ApaI-EcoRV site. Loxp sites were inserted after exon 1 and before exon 4 of the *Spp1* locus to engineer removal of exons 2 and 3 and generate a premature stop codon.

*Generation of Spp1 floxed dystrophic mice*

*Spp1 floxed* mice were generated by Mouse Biology Program at University of California, Davis. Targeting vector for floxed *Spp1* was electroporated into ES cells of C57BL/6N strain. Neomycin resistant cells were selected and microinjected into blastcysts of Balb/C strain. Mice with germline transmission were bred with FLP mice (C57BL/6N-Tg(CAG-Flpo)1Afst/Mmucd, provided from Mutated Mouse Resource & Research Center at University of California, Davis). Pups in which neomycin gene was excised were selected and bred. *Spp1* floxed mice were crossed to C57BL/10ScSn-Dmd$^{mdx}$/J (Jax #001801) mice were obtained by The Jackson Laboratories.

*Crossing of Spp1 floxed mice with tissue-specific Cre-mdx mice*

*Lyz2-Cre* (B6.129P2-Lyz2$^{tm1(cre)Ifo}$/J, Jax #: 004781) for myeloid-specific Cre was obtained from The Jackson Laboratories and crossed to *Spp1* floxed *mdx* mice.

PCR for genotyping myeloid-specific *Spp1* conditional knockout mice

PCR genotyping of Lyz2cre mice used the following primers: (Lyz2 mutant: 5'- CCC AGA AAT GCC AGA TTA CG-3'; Lys2 common: 5' CTT GGG CTG CCA GAA TTT CTC-3'; Lys2 WT: 5'-TTA CAG TCG GCC AGG CTG AC-3'). PCR for the floxed *Spp1* allele used the following primers: (Forward: 5'- GGA CCT TGA GTG ACT GGT TCT-3'; Reverse: 5'- TGG ACC TGA ACT CTG TGT GC-3')

*Cell isolation for single-cell RNAseq*

Mice were sacrificed and muscles from arms and hindlimbs (triceps, quadriceps, tibialis anterior, gastrocnemius) and diaphragm were pooled into a Petri dish containing sterile PBS (with $Ca^{2+}$, $Mg^{2+}$) for weighing. Muscles were washed in PBS (with $Ca^{2+}$, $Mg^{2+}$) and then minced in a 1:5 (weigh:volume) solution of 6mg/mL collagenase type 2 (Worthington Biochemical Corp.). To further digest the tissue, we transferred the tissue and collagenase solution to a 50mL conical tube in which we added a 1/1000 volume of DNAse I (final 20kunitz/mL) and placed at 37°C. Once the tissue was digested, the mixture was filtered through a 70um nylon filter and was washed with $Ca^{2+}$, $Mg^{2+}$-free PBS making sure not to add more than 1g muscle per tube. Cells were pelleted by centrifugation at (330xg) for 5 minutes. After discarding the supernatant and breaking up the pellet with 5mL of $Ca^{2+}$, $Mg^{2+}$-free PBS, we filled the conical tube with $Ca^{2+}$, $Mg^{2+}$-free PBS and centrifuged again for 10 minutes. We used a Cell Debris Removal kit (Miltenyi) and centrifuged at (300xg**)** at 4°C. After removing the PBS and interphase (cell debris) layers, cells were washed with $Ca^{2+}$, $Mg^{2+}$-free PBS and centrifuged again at (3000xg) at 4°C. Cells were resuspended in ACK lysis buffer (Lonza) to lyse red blood cells and centrifuged at (300xg) at 4°C for 10 minutes. Pellet was resuspended in $Ca^{2+}$, $Mg^{2+}$-free PBS and cells were filtered with a 40um nylon filter and washed with additional $Ca^{2+}$, $Mg^{2+}$-free PBS. After centrifugation (300xg) at 4°C, we used a Dead Cell Removal Kit. The purified cell solution

was centrifuged at (300xg) at 4°C. We discarded the supernatant and resuspended the cell pellet in a 0.04% BSA solution. To count cells, a small sample volume was mixed 1:1 with 0.4% Trypan blue solution and counted using a hemocytometer.

*Macrophage isolation for bulk RNAseq*

Macrophage isolation similar to the above protocol until the last centrifugation step before Dead Cell Removal Kit. Cells were blocked using a purified anti-CD16/32 (1:100, Biolegend), F4/80-PE (1:50, eBiosciences) antibody.

*scRNAseq library construction, sequencing and data analysis*

scRNAseq was conducted on cells isolated from murine skeletal muscle. Libraries were constructed using the Chromium Single Cell 3' Reagent Kits v3 (10X Genomics) at the UCLA Technology Center for Genomics & Bioinformatics (TCGB). cDNA libraries were sequenced on the NextSeq500 High Output platform using to achieve approximately 20,000 reads/cell. Sequencing reads were processed using the 10X Genomics Cell Ranger (Seurat version 3.0) was used.

*Flow sorting and cytometry*

Stromal cells from myeloid-specific Spp1 cKO and control mice were isolated, dissociated and minced in 500U/mL collagenase II (Worthington) and incubated at 37°C and slowly rocked for 30 minutes. Muscles were washed with DPBS(-/-) + 10% PBS and centrifugated at (600xg). Minced muscles were further dissociated in a solution consisting of 1.5U/mL collagenase D (Roche) and 2.4U/mL dispase (Worthington) and incubated and slowly rocked for 45 minutes. Dissociated cells were then filtered using 40um cell strainers. Hoescht 33342 (Tocris, 2mg/mL) was used for live cell discrimination and treated with Fc block (CD16/32) (Biolegend). The cells were then stained using the following primary antibodies :

CD45-FITC (1:500, eBiosciences), CD31-FITC (1:300, eBiosciences), ITGA7 (1:300, R&D), SCA1-PerCP-Cy5.5 (1:300, Biolegend), CD26-PE (1:1000, Biolegend), LIFR-PE-Cy7 (1:300, Biolegend), CD201-APC (1:200, Biolegend) for 45 minutes at 4°C. FAPs, Lifr(+) and Procr(+) cells were isolated using a FACSAria II sorted (BD Biosciences) into DMEM media.

*Bulk RNAseq*

For macrophage bulk RNAseq total RNA was isolated using the Zymo Quick RNA Micro Prep Kit. RNA libraries were prepared by the UCLA TCGB Core and sequencing was performed on NextSeq500 Mid Output. For stromal cell bulk RNAseq total RNA was isolated and RNA libraries were prepared by the UCLA TCGB Core. Sequencing was done on the NovaSeq X Plus 10B.

*Muscle dissection, freezing and histology*

Muscles were dissected, covered with Tissue-Tek OCT mounting media and frozen in liquid nitrogen-cooled isopentane. 10um sections were cut on a cryostat (Leica CM1860 UC) and stored at -20°C until immunostaining or histological staining. Muscle cryosections were fixed in 4% paraformaldehyde for 10 minutes, treated with 0.3% $H_2O_2$ for 5 minutes, then incubated with a 5% True Black solution (Biotium in 70% ethanol). Sections were blocked with IHC buffer (5% Tween-20, 3% BSA, 0.02% gelatin in PBS) for 1 hour. Primary antibodies were as follows: PDGFRA (1:200, R&D Systems), CEBPD (1:100, Abcam), Laminin (1:200, R&D Systems), Perilipin1 (1:100, Thermo).

*Oil Red O staining*

10um diaphragm muscle sections were air dried for 30 minutes, then fixed with 10% PFA for 10 minutes. After washing with running tap water for 1 minute, the sections were

submerged in 60% isopropanol and incubated in a 60% Oil Red O working solution in dd$H_2O$ (v/v) for 15 minutes. Slides were washed with 60% isopropanol and subsequently submerged in hematoxylin for 1 minute. Finally, sections were mounted using VECTASHIELD (Vector Laboratories) and imaged using brightfield microscopy on the AxioImager.M1 (Zeiss).

*Wire mesh test*

Murine muscle strength was assessed using a wire mesh test previously described (Capote et al. 2016). In short, this custom-built apparatus consists of a wire mesh screen pulled over a wooden frame that can be rotated 180° on a swivel. Mice were placed in the middle of the screen and rotated such that they were hung upside down over a container, 10 inches below. Hang time was recorded for each of the five trials (with 1 minute of rest time in between each trial) and the mean hang time was calculated for each mouse and normalized for body weight.

*Fractionation of crosslinked and non-crosslinked collagen*

To fractionate non-crosslinked and crosslinked collagen within muscle tissue, we adapted a collagen solubility assay. Frozen muscle tissue was ground in a mortar and pestle over dry ice and weighed. Ground tissue was washed in 1mL of PBS and rotated for 30 minutes at 4°C. Samples were then centrifuged at 16,000g for 30 minutes at 4°C. The non-crosslinked collagen in the pelleted tissue was then digested in a 1:6 (weight:volume) solution of 0.5M acetic acid and 1mg/mL pepsin and rotated overnight at 4°C. Samples were centrifuged at 16,000g for 30 minutes resulting in a pepsin-soluble fraction (PSF, supernatant) and pepsin-insoluble fraction (PIF, pellet). The PSF was further processed by adding a 1:1 volume of 4M NaCl and was rotated for 30 minutes at 4°C. After centrifuging the PSF at 16,000g for 30 minutes at 4°C, the supernatant was discarded. Collagen was then quantified in the PSF and PIF pelleted fractions by a hydroxyproline assay.

*Hydroxyproline assay*

To quantify the collagen contents of the PSF and PIF fractions, we adapted a hydroxyproline assay. The PSF and PIF were hydrolyzed with 0.5mL and 1mL of 7M NaOH, respectively, and transferred to 12-mL glass screw thread culture tubes (DWK Life Sciences). Tube caps were closed tightly and vortexed to bring fractions to the bottom. Samples were autoclaved for 45 minutes at 250°C liquid cycle. Hydrolysates were immediately vortexed after autoclaving. 0.5mL or 1mL of 3.5M H2SO4 was added to the PSF and PIF, respectively, immediately vortexed and transferred to 1.5mL Eppendorf tubes. These samples can be kept at 4°C overnight if needed. For measurement, we made triplicates of 25-50uL of each sample/standard. We added 0.45mL Choloramine-T and incubated at room temperature for 25 minutes, covered in foil to protect from light. 500uL Ehrlich reagent was added and incubated in a water bath at 65°C for 20 minutes. Absorbance was measured at 560nm using a spectrophotometer.

RESULTS

*Generation of Spp1 conditional knock out*

To assess the effect of macrophage derived *Spp1* on the dystrophic niche, we generated a myeloid specific *Spp1* conditional knockout mouse line (MΦ cKO) using the *Lyz2*$^{cre}$ (also known as *LyzM*$^{cre}$) driver to specifically excise Spp1 from myeloid cells. These *Lyz2*$^{cre}$ mice were crossed to *Spp1 fl/fl* mice congenic to the *mdx* BL/10 background which, after excision of exons two and three, induced a premature stop codon at the *Spp1* locus.

*Effect of macrophage-derived Spp1 on cellular frequencies and phenotypes in the dystrophic niche*

To determine how macrophage derived *Spp1* impacts cellular profiles within dystrophic muscle, we isolated single cell homogenates from limb and diaphragm muscle from 3-month-old MΦ cKO (n=3) and control (n=3) mice and created scRNAseq libraries using 10x Genomics. Using Seurat analysis, we analyzed 10,657 cells from MΦ cKO muscle and 7,156 cells from control muscle revealing nine major cell types (Figure **2.1A,B**). The major cell types we isolated include stromal cells and a variety of immune cells such as macrophages, neutrophils, T-cells and B-cells. We also isolated cells from the vasculature such as red blood cells (RBC), endothelial cells and smooth muscle cells (SMC) as well as nerve cells, indicative of remnants of neuromuscular junctions. Strikingly, we noted the absence of a stromal cell type (cluster 6) (**Figure 2.1C**) by UMAP, however there was no difference in the percentage of stromal cells in MΦ cKO compared to control muscle (**Figure 2.1D**). This suggests that macrophage derived *Spp1* has a paracrine effect on stromal cell heterogeneity.

While macrophages are the main source of Spp1, our lab has shown that it is expressed by a variety of cell types within the muscle niche (data not shown). Our scRNAseq showed that *Spp1* is expressed by several cell types in dystrophic muscle with macrophages being the primary source (**Figure 2.1C**). Analysis of the macrophage clusters validated that *Spp1* was significantly reduced in cells from MΦ cKO mice compared to control (**Figure 2.1D**). We further analyzed how these cellular profiles changed by genotype and found that there was a difference in other immune cell types (**Figure 2.1C,D**). We previously showed that global *Spp1* knockdown correlated with a significant decrease in neutrophils in 4-week-old muscle[18]. Here we showed that ablation of macrophage-derived *Spp1* resulted in decreased neutrophils, as well as reduced T- and B-cells. Intriguingly, we observed a three-fold increase in the proportion of macrophages compared to control muscle suggesting an autocrine effect of *Spp1*. Overall, we showed that the loss of Spp1 from macrophages, specifically (**Figure 2.1E**), is having an autocrine and paracrine effect on the muscle milieu.

*Autocrine effect of macrophage derived Spp1 on macrophage heterogeneity and phenotypes*

To better understand the autocrine effect of macrophage-derived *Spp1* on macrophage subtypes, we conducted unsupervised subclustering of the macrophage populations and identified eight distinct subtypes: two monocyte populations, four macrophage populations, and two dendritic cell populations (**Figure 2.2A**). Monocyte cluster 1 and 2 marked by *Plac8* expression. Resident M2-like macrophages marked by *Mrc1* (CD206), *Mertk*, *Fcgr1* (CD64) and MHCII genes like *H2-Aa* and *H2-Eb1* increased in the MΦ cKO compared to control. Macrophage cluster 1 and 3 both express *Spp1,* which we previously showed is a marker of M2c macrophages. However, cluster 1 is marked by high *Thbs1* expression and *Arg1* suggesting an M2a-like profile while cluster 3 has high expression of *Lgals3* and *Igf1* suggesting an M2c-like profile as seen previously (**Figure 2.2B**). While the proportion of cluster 1 remained steady in the MΦ cKO we saw a mild increase in the M2c-like population (**Figure 2.2C,D**). In contrast, M1-like macrophages (cluster 2) a population marked by *Il1b*, decreased with macrophage-derived *Spp1* ablation. Analysis of the proportion of the four macrophage populations alone showed that there was a 1.4-fold increase in the M2:M1 macrophage ratio in the MΦ cKO (**Figure 2.2E**) suggesting that macrophage-derived Spp1 has an autocrine effect on macrophage polarization away from an M1-like phenotype.

We validated these results by isolating macrophages from MΦ cKO and *mdx* mice by FACS using F4/80 as a selection marker. We analyzed significant differentially expressed genes of sorted cells by bulk RNAseq and found that F4/80(+) cells from MΦ cKO showed an increase in many M2-like markers and decrease in M1-like markers (**Figure 2.2F**). Specifically, we saw 1.6-fold increase in *Cd163* expression and a two-fold decrease in *Arg1* expression compared to mdx control. Our lab previously showed that M2a-like macrophages expressed high levels of *Arg1* while M2c-like showed the highest expression of *Spp1*[34]. Our data suggests that the macrophage phenotype from MΦ cKO is shifted more towards an M2-like state and more

specifically an M2c-like macrophage transcriptional profile, which correlates with our scRNAseq data.

Interestingly, we noticed that *Ltbp4* expression was significantly reduced in F4/80(+) cells from MΦ cKO compared to control (**Figure 2.2F**). Ltbp4 is known to be a modifier of TGFβ signaling[36], specifically TGFβ1 secretion and activity[42]. This was intriguing as previous studies have shown that Spp1 is a modifier of TGFβ[19]. While we did not see expression of *Ltbp4* in our scRNAseq data, instead we observed a decrease in *Tgfb1* expression in M2a-like macrophages and monocyte 1 cluster (**Figure 2.2G**). Our data suggests that macrophage-derived Spp1 has an autocrine effect of reducing macrophage-derived *Tgfb1* (**Figure 2.2H**).

*Identification of novel adipogenically-primed stromal cell populations impacted by MΦ-Spp1*

One of the most striking differences observed in the single cell sequencing data was a severe reduction of a stromal cell population in the MΦ cKO. To better understand the heterogeneity of these stromal cell populations we further subclustered stromal cells (all PDGFRA+) and identified five transcriptionally distinct clusters (**Figure 2.3A**). Three of which showed transcriptional profiles of known stromal cell types such as fibroadipogenic progenitor cells (FAPs, cluster 0) marked by *Ly6a* (SCA1) and *Cd34*, a traditional fibroblast population (cluster 1) that is enriched in a variety of collagen genes such as *Col3a1*, *Col4a2* and *Col6a2* and showed the highest expression of *Pdgfra* as well as an activated fibroblast population identified by expression of *Postn* and *Acta2* (cluster 3). We also identified a *Tnmd*(+) tenocyte population (cluster 5).

Our analysis showed that the previously mentioned novel population (**Fig. 2.1B**) subclustered further into two stromal cell populations: one which we call *Lifr*$^+$ (cluster 2) and the other *Procr*$^+$(cluster 4) (**Figure 2.3A,B**). Interestingly, both the *Lifr*$^+$ and *Procr*$^+$ stromal cell populations drastically contract in the MΦ cKO compared to control muscle (**Figure 2.3C,D**) while the FAPs, traditional fibroblasts and activated fibroblasts expand in the MΦ cKO. This

observation suggests that macrophage derived *Spp1* may regulate either a stromal cell subtype switch or survival of these previously uncharacterized stromal cell populations.

To validate the presence of these novel stromal cell populations *in vivo*, we designed a FACS sorting strategy based on the single cell RNAseq markers to isolate the cells from skeletal muscle (**Figure 2.4A,B**). We used SCA1 (*Ly6a*) and DPP4, which were highly expressed in the FAP population, to isolate FAPs while SCA1$^{+}$/DPP4$^{-}$ cells were further sorted by LIFR and PROCR expression to isolate the Lifr$^{+}$ and Procr$^{+}$ populations (**Figure 2.4B**). Bulk RNAseq analysis validated preferential expression of key markers identified by scRNAseq like *Pi16* and *Cd34* in isolated FAPs whereas Lifr$^{+}$ and Procr$^{+}$ cells showed higher expression of *Sox4* and *Apod* (**Figure 2.4C**). The ability to sort these cells and validation of markers identified by scRNAseq lends strong support for these cells as a novel population of stromal cells. Together, these data suggest the presence of two previously unidentified skeletal muscle-resident Lifr$^{+}$ and Procr$^{+}$ stromal cell subtypes *in vivo*.

To better understand the cellular dynamics of these stromal cell populations we conducted RNA velocity, which models splicing kinetics from scRNAseq data to predict future cell states[44] (**Figure 2.4D**). Arrows in the FAPs (cluster 0, pink) suggest a self-renewing population that also can give rise to the traditional fibroblast population (cluster 1, gold). Interestingly we see that spatially on the UMAP, the Lifr$^{+}$ (cluster 2, green) and Procr$^{+}$ (cluster 4, dark blue) populations are separated from the other stromal cell clusters suggesting a more transcriptionally distinct population. Lifr$^{+}$ and Procr$^{+}$ cell states transition within these populations and maybe even converge with FAPs to give rise towards the fibroblast population. However, we do not see evidence of a transitional state from the FAPs and fibroblast population towards Lifr$^{+}$ and Procr$^{+}$ cells.

*Identification of macrophage-derived Spp1 as a regulator of macrophage-stromal cell crosstalk*

Because we observed loss of stromal cells in the MΦ cKO, we asked whether macrophage-derived Spp1 is an upstream regulator of macrophage-stromal cell crosstalk. To address this question, we computationally investigated possible interactions between ligands released from macrophages and target genes in the novel stromal cell population (**Figure 2.1B**) using NicheNet analysis. This analysis created a prioritized list of ligand-target links from differentially expressed genes in our scRNAseq dataset. The top prioritized ligand regulating gene expression in this stromal cell population was predicted to be TGFβ1 (**Figure 2.5**). Interestingly, we also saw Spp1 as a top ranked ligand influencing stromal cell target gene expression.

*Ablation of macrophage-derived Spp1 regulates adipogenically primed stromal cell populations involved in intramuscular fat accumulation*

To further understand the phenotype of *Lifr*$^{+}$ and *Procr*$^{+}$ subpopulations we carried out gene set enrichment analysis using markers from the scRNAseq data set. We saw that both the *Lifr*$^{+}$ and *Procr*$^{+}$ cells are enriched in genes involved in adipogenesis such as *Cebpd*, a master regulator of adipogenesis, *Lifr* and *Fabp4*, which have been shown to be upregulated during adipocyte differentiation[45–47] (**Figure 2.6A,B**). This suggested that these stromal cell subsets may be adipogenically-primed and could play a critical role in fat accumulation within the muscle. Analysis of significant differentially expressed genes by bulk RNAseq from isolated stromal cell populations validated an increased expression of adipogenesis markers in the Lifr$^{+}$ and Procr$^{+}$ clusters compared to FAPs (**Figure 2.6C**). We also see enrichment of genes involved in TGFβ and IGF-1 signaling, which is also reflected in the gene set enrichment analysis. Interestingly, the expression of *Spp1* is increased in Lifr$^{+}$ and Procr$^{+}$ cells compared to control suggesting a preferential paracrine role of macrophage-derived Spp1 on Spp1 expressed in these adipogenically primed stromal cell subpopulations.

To assess if loss of Lifr$^+$ and Procr$^+$ subpopulations have an effect on fat accumulation in dystrophic muscle, 6-month-old diaphragm muscles from MΦ cKO and control mice with Perilipin, a marker of mature adipocyte. Immunofluorescence analysis showed evidence of a significant decrease in MΦ cKO diaphragms compared to control, but quantification is necessary (**Figure 2.7A**). To validate this, we stained 3-month and 6-month-old diaphragm muscle with Oil Red O which identifies neutral triglyceride and lipid droplets often associated with adipocytes. We saw a significant decrease in the percentage of Oil Red O area staining in 3-month-old MΦ cKO diaphragm muscles compared to control (**Figure 2.7B**). 6-month-old diaphragms in MΦ cKO mice also showed that the Oil Red O area was uniformly, but mildly decreased compared to control, which had up to 6-times the amount found in the 3-month-old controls (**Figure 2.7C**). This data suggests that ablation of macrophage derived Spp1 plays a role in regulation of intramuscular fat accumulation.

## DISCUSSION

In this study we conducted an unbiased scRNAseq transcriptomic analysis of dystrophic muscle to unravel the impact of ablation of macrophage-specific Spp1 on cell-cell interactions. We found that Spp1 from macrophages promotes an autocrine loop that induces macrophage-specific TGFβ expression, specifically in M2a-like macrophages. We showed that this loop polarizes macrophages away from a pro-inflammatory phenotype. Predicted ligand-target gene network analysis identified macrophage-specific TGFβ1 as the top regulator of gene expression in stromal cells, suggesting significant cross talk between these two cell types. In addition, we saw that loss of TGFβ1 leads to loss of two unique stromal cell populations, called Lifr$^+$ and Procr$^+$ cells, that have pro-adipogenic profiles, correlating with significantly reduced fat accumulation in 3-month-old diaphragms.

Considering that macrophages are the main source of Spp1, it is important to understand how Spp1 from macrophages alters cellular dynamics in dystrophic muscle. We previously showed that global knockout of *Spp1* in *mdx* mice had an overall increase in the M2:M1 ratio driven by expansion of the M2c-like macrophages and a concomitant reduction in the M1-like and M2a-like macrophages[34]. Our data confirms that macrophage-derived Spp1 is a critical source that regulates macrophage polarization away from an M1-like state. Additionally, our bulk RNAseq of isolated F4/80$^{+}$ macrophages further identified that macrophage-specific Spp1 has an autocrine effect on macrophage transcriptional profiles inducing anti-inflammatory markers and mitigating pro-inflammatory gene expression.

An important finding from this study is the identification and characterization of two novel stromal cell populations in dystrophic muscle. Prior research has considered FAPs to be the only mesenchymal progenitor cell that gives rise to adipocytes[43]. Much of the current literature investigating FAPs in muscle have sorted PDGFRA$^{+}$ cells, a pan marker for stromal cells, and have studied their impact on myofiber regeneration, fibrosis and IMAT accumulation[48–51]. However, other studies have further characterized FAPs as Lin$^{-}$ (CD45$^{-}$CD31$^{-}$ITGA7$^{-}$) SCA1$^{+}$CD34$^{+}$ cells. Our data uses an unbiased approach that further clarifies the literature by identifying five transcriptionally-distinct stromal cell populations that have varying expression levels of *Pdgfra*, *Ly6a*, and *Cd34*. We found that there is a spectrum of stromal cell subtypes that may play different roles affecting the dystrophic process. We showed that we could sort and isolate FAPs, Lifr$^{+}$ and Procr$^{+}$ stromal cells using unique markers identified from scRNAseq from other stromal cell subtypes. Thus, an important finding of these studies is the identification of two novel stromal cell populations.

It is widely known that IMAT accumulation occurs in DMD patient muscles and it has been shown that fat infiltration correlates with age and clinical performance evaluations[52–54]. This has long been assumed to be due to the chronic presence and buildup of FAPs that are reprogrammed by the microenvironment to differentiate towards an adipogenic fate. Our data

suggest that Lifr+ and Procr+ cells are either completely or partially responsible for fat accumulation in dystrophic muscles. scRNAseq and bulk RNAseq of isolated stromal cell populations confirmed that $Lifr^+$ and $Procr^+$ cells are enriched in adipogenic markers compared to FAPs suggesting cell types primed towards a pro-adipogenic fate. While RNA velocity showed evidence that these cells may be a separate, distinct stromal cell subtype rather than a transient FAP differentiation cell state towards an adipogenic fate, lineage tracing analysis is needed to identify the origin of these novel subtypes.

Both Spp1 and TGFβ signaling are implicated in modifying DMD disease progression[36]. Our lab and others have showed a relationship between Spp1 and TGFβ in dystrophic muscle, but no studies to our knowledge have identified the cell type(s) involved[18,55]. Our data clarifies a specific autocrine *Spp1-Tgfb1* relationship within macrophage subpopulations where a pan-macrophage reduction in *Spp1* results in a significant reduction in *Tgfb1*, specifically in M2a-like macrophages.

In acute muscle injury, crosstalk between macrophages and other cells in the niche are carefully orchestrated to ensure proper muscle regeneration. Specifically, the progression from a TNF-enriched microenvironment, induced by M1-like macrophages, to a TGFβ-enriched microenvironment, induced by M2-like macrophages, as crucial for regulating a transient increase in stromal cells that structurally support regeneration[39,56]. In DMD, however, chronic cycles of injury create a persistent overlap of both cytokines. This continued presence of pro-survival TGFβ signal counteracts pro-apoptotic TNF signals leading to failed regeneration and pathological fibrosis[42,56]. Our data show that while there is persistence of both M1-like and M2-like macrophages, this reduction in macrophage TGFβ1 may be critical in reaching a less aberrant fibro-inflammatory response. Interestingly, in contrast to known literature, we show that TGFβ1 may act as a pro-survival signal for adipogenically primed stromal cells rather than pro-fibrotic stromal cell populations[56]. Additionally, we observed that reduced macrophage TGFβ1 is correlated with increased FAPs, traditional fibroblasts and activated fibroblasts. Furthermore, we

saw no difference in overall collagen content and a reduction in crosslinked collagen with loss of macrophage-derived *Spp1* and reduced *Tgfb1*. Instead, we quantified a significant reduction of fat accumulation in diaphragms from 3-month-old mice and a mild, but more uniform reduction at 6-months.

In conclusion, this study provides a deeper understanding of SPP1 biology and its role in both autocrine and paracrine communication pathways in immune regulation and fibrogenic responses in DMD.

ACKNOWLEDGEMENTS

We thank Jane Wen, Diana Becerra, Jesus Perez and Bradley Smith for technical assistance. We thank the UCLA Technology Center for Genomics & Bioinformatics and the UCLA Jonsson Comprehensive Cancer Center Flow Cytometry Core, specifically Trent Su, Salem Haile and Iris Williams, for sequencing, access to equipment and analysis for this study. We extend our immense gratitude to Dr. Armando Villalta, Philip Kamal Farahat and Saba Movahedi from UCI for their intellectual and technical expertise that helped propel this project forward. This work was support in part by a Howard Hughes Medical Institute Gilliam Fellowship (GT11023) to R.A. and M.S., the UCLA Muscle Biology, Pathophysiology, and Therapeutics Training Program (NIH NIAMS T32 AR065972) to R.A., and NIH-NINDS R01NS117912, NIH-NIAMS P50 AR052646, DOD MD190060 (to MS), and NIH NINDS RO1 NS120060 (to SV).

FIGURES

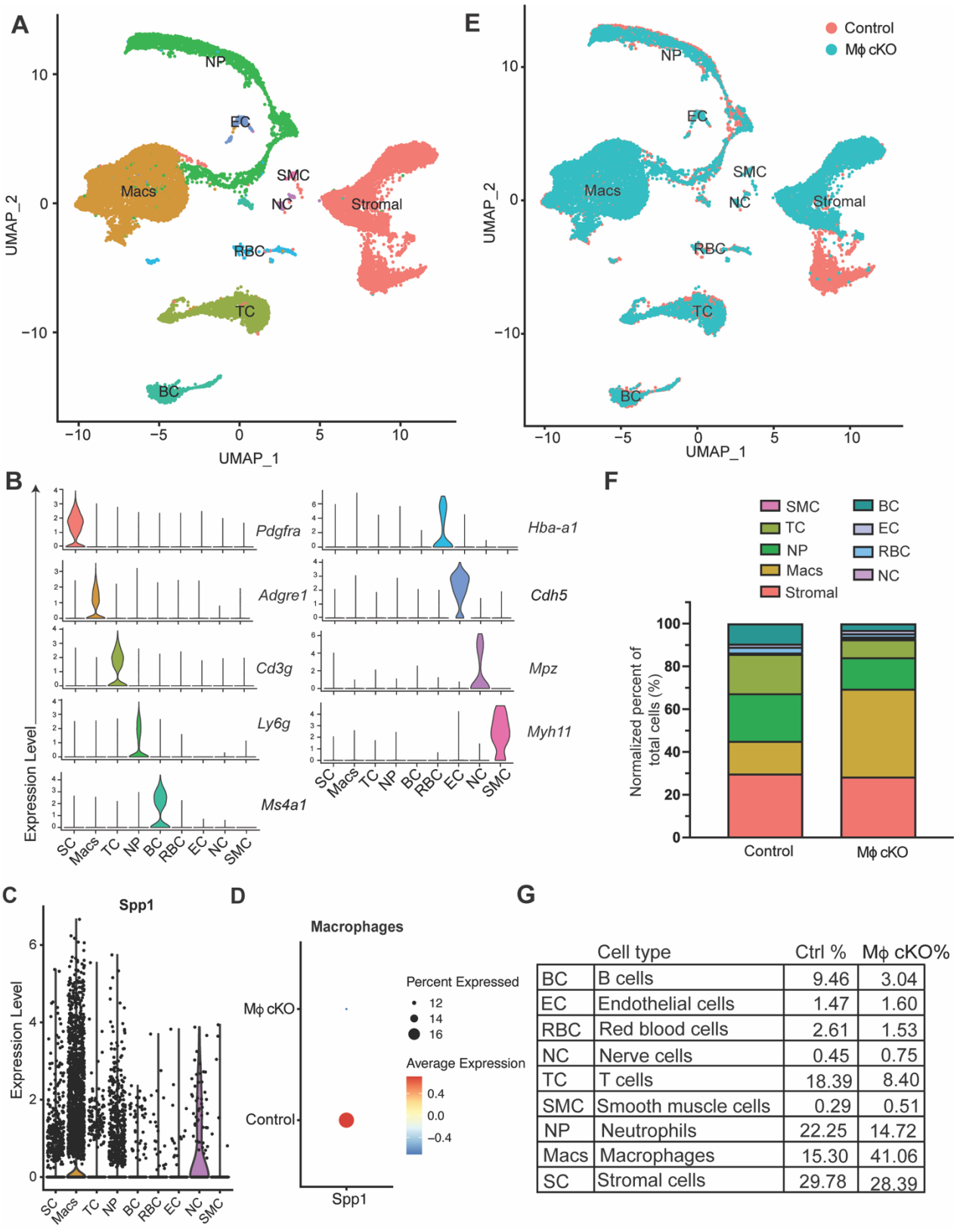


G

| | Cell type | Ctrl % | Mϕ cKO% |
|---|---|---|---|
| BC | B cells | 9.46 | 3.04 |
| EC | Endothelial cells | 1.47 | 1.60 |
| RBC | Red blood cells | 2.61 | 1.53 |
| NC | Nerve cells | 0.45 | 0.75 |
| TC | T cells | 18.39 | 8.40 |
| SMC | Smooth muscle cells | 0.29 | 0.51 |
| NP | Neutrophils | 22.25 | 14.72 |
| Macs | Macrophages | 15.30 | 41.06 |
| SC | Stromal cells | 29.78 | 28.39 |

**Figure 2.1. scRNAseq reveals Mϕ Spp1 has paracrine effect on stromal cell heterogeneity and autocrine effect on macrophage cellular frequencies.**

(A) UMAP plot shows unsupervised clustering of cells isolated from 12-week-old MΦ cKO and control skeletal muscle (n=3 per genotype).

(B) Violin plots of representative markers used in cell type annotation.

(C) Violin plot of expression level of *Spp1* across all cell types shown in (A).

(D) Dotplot showing loss of macrophage-derived *Spp1* in cells isolated from MΦ cKO muscle compared to control.

(E) UMAP plot depicting distribution of cells isolated from MΦ cKO (blue) and control (pink) skeletal muscle (n=3 per genotype).

(F,G) Proportion of each cell type (normalized to total cells) and how they change by genotype.

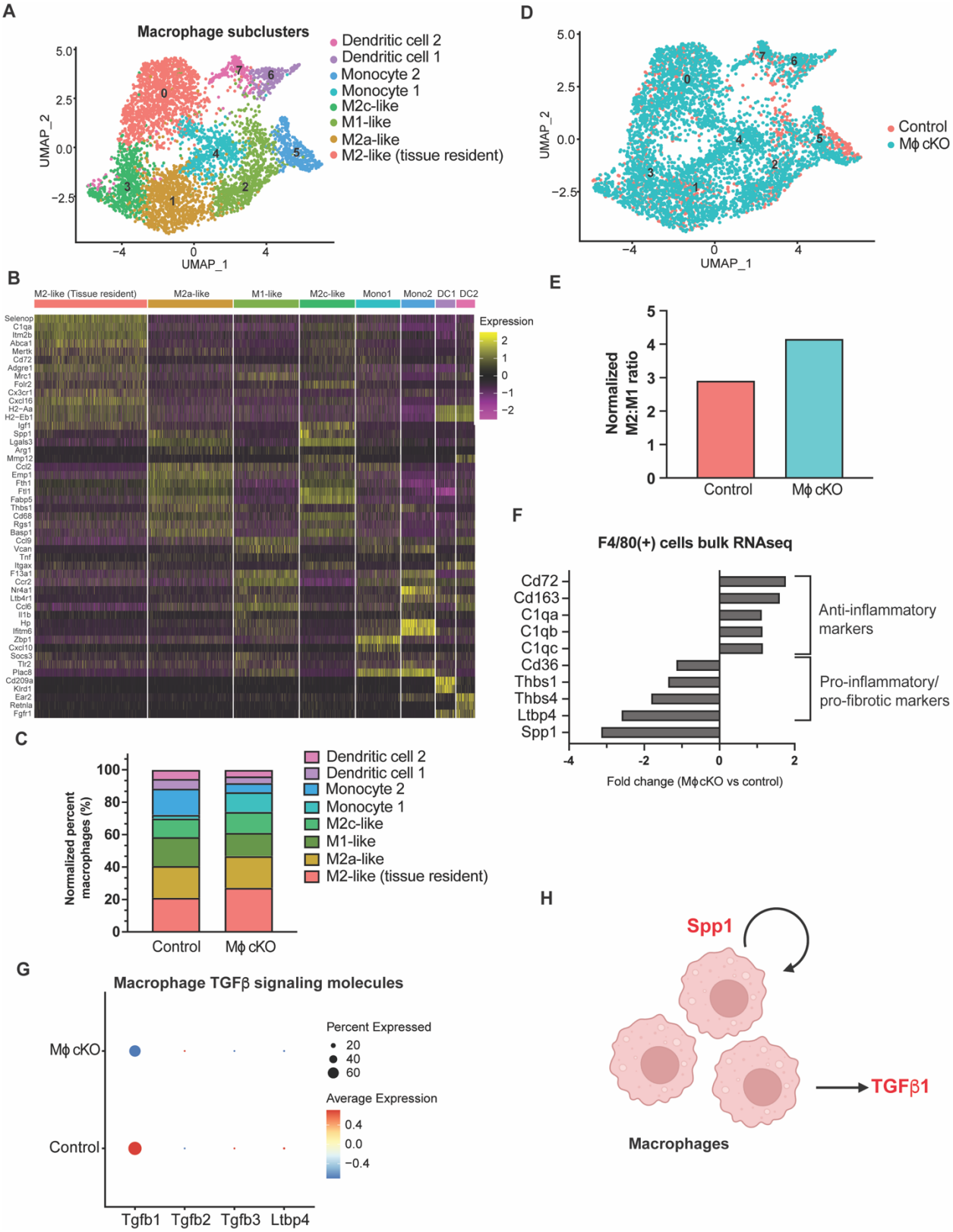
A
Macrophage subclusters
Dendritic cell 2
Dendritic cell 1
Monocyte 2
Monocyte 1
M2c-like
M1-like
M2a-like
M2-like (tissue resident)
UMAP_1
UMAP_2
D
Control
Mϕ cKO
B
M2-like (Tissue resident)
M2a-like
M1-like
M2c-like
Mono1
Mono2
DC1
DC2
Expression
E
Normalized M2:M1 ratio
Control
Mϕ cKO
C
Normalized percent macrophages (%)
F
F4/80(+) cells bulk RNAseq
Cd72
Cd163
C1qa
C1qb
C1qc
Cd36
Thbs1
Thbs4
Ltbp4
Spp1
Anti-inflammatory markers
Pro-inflammatory/ pro-fibrotic markers
Fold change (MϕcKO vs control)
G
Macrophage TGFβ signaling molecules
Mϕ cKO
Control
Tgfb1
Tgfb2
Tgfb3
Ltbp4
Percent Expressed
Average Expression
H
Spp1
TGFβ1
Macrophages

**Figure 2.2. Macrophage subcluster analysis reveals autocrine regulation of macrophage-derived Spp1 on macrophage phenotype.**

(A) UMAP plot shows unsupervised clustering of macrophage cell subpopulations from MΦ cKO and control skeletal muscle.

(B) Heatmap of top gene cluster markers from each subpopulation.

(C) Proportion of each subpopulation (normalized to total macrophage cells) by genotype.

(D) UMAP plot shows unsupervised clustering of macrophage cell subpopulations from MΦ cKO (blue) and control (pink) skeletal muscle

(E) Ratio of M2:M1 macrophage populations (cluster 0, 1, 2, 3) by genotype.

(F) Fold change of significant differentially expressed inflammatory/fibrotic markers in from FACS isolated F4/80$^{+}$ cells from MΦ cKO compared to control skeletal muscle.

(G) Dotplot of TGFβ ligands and regulators in all macrophage subclusters by genotype.

(H) Schematic of autocrine regulation of macrophage-derived Spp1 on macrophage-specific TGFβ1 expression.

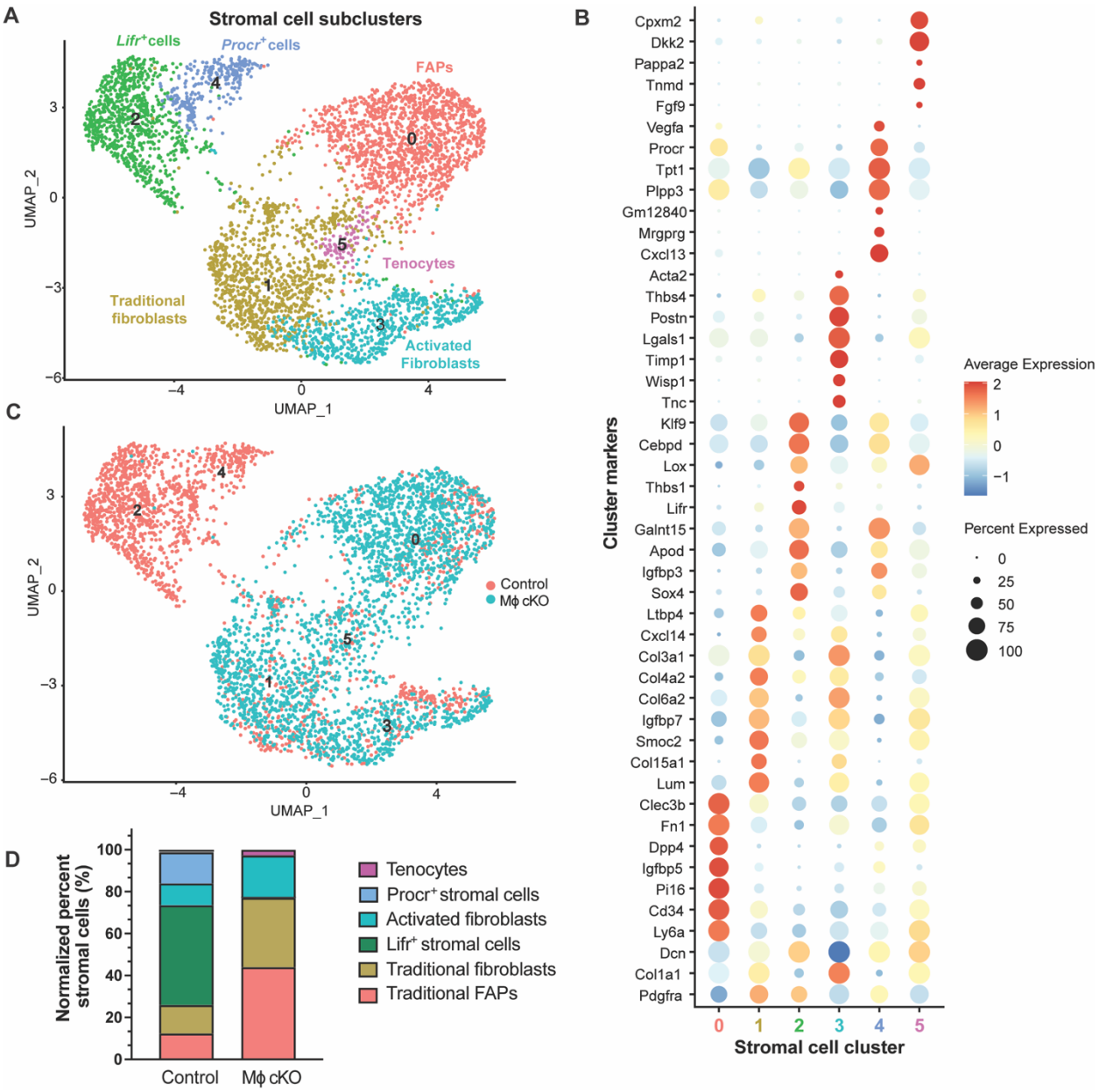
A
Stromal cell subclusters
Lifr+ cells
Procr+ cells
FAPs
Tenocytes
Traditional fibroblasts
Activated Fibroblasts
UMAP_1
UMAP_2
B
Cpxm2
Dkk2
Pappa2
Tnmd
Fgf9
Vegfa
Procr
Tpt1
Plpp3
Gm12840
Mrgprg
Cxcl13
Acta2
Thbs4
Postn
Lgals1
Timp1
Wisp1
Tnc
Klf9
Cebpd
Lox
Thbs1
Lifr
Galnt15
Apod
Igfbp3
Sox4
Ltbp4
Cxcl14
Col3a1
Col4a2
Col6a2
Igfbp7
Smoc2
Col15a1
Lum
Clec3b
Fn1
Dpp4
Igfbp5
Pi16
Cd34
Ly6a
Dcn
Col1a1
Pdgfra
Cluster markers
Stromal cell cluster
Average Expression
Percent Expressed
C
Control
Mϕ cKO
D
Normalized percent stromal cells (%)
Tenocytes
Procr+ stromal cells
Activated fibroblasts
Lifr+ stromal cells
Traditional fibroblasts
Traditional FAPs
Control
Mϕ cKO

**Figure 2.3. Stromal cell subcluster analysis reveals stromal cell heterogeneity regulated by macrophage-derived *Spp1*.**

(A) UMAP plot shows unsupervised clustering of stromal cell subpopulations from MΦ cKO and control skeletal muscle.

(B) Dotplot of top cluster markers used to identify stromal cell subtypes.

(C) UMAP plot distribution of stromal cells from each genotype, MΦ cKO (blue) and control (pink).

(D) Proportion of each cell type (normalized to total stromal cells) by genotype.

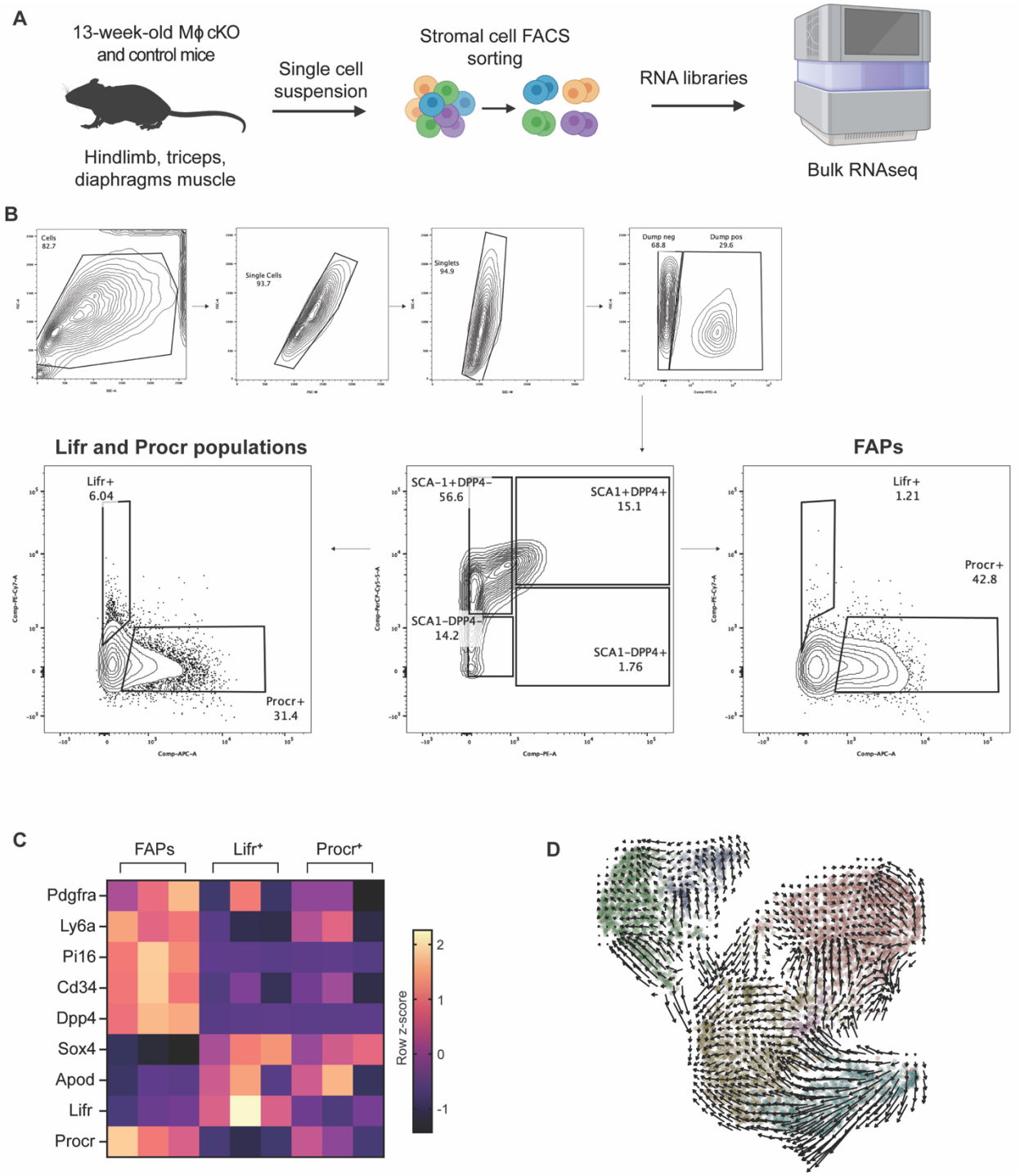
A
13-week-old Mϕ cKO and control mice
Hindlimb, triceps, diaphragms muscle
Single cell suspension
Stromal cell FACS sorting
RNA libraries
Bulk RNAseq
B
Cells 82.7
Single Cells 93.7
Singlets 94.9
Dump neg 68.8
Dump pos 29.6
Lifr and Procr populations
Lifr+ 6.04
Procr+ 31.4
SCA-1+DPP4- 56.6
SCA1+DPP4+ 15.1
SCA1-DPP4- 14.2
SCA1-DPP4+ 1.76
FAPs
Lifr+ 1.21
Procr+ 42.8
C
FAPs
Lifr+
Procr+
Pdgfra
Ly6a
Pi16
Cd34
Dpp4
Sox4
Apod
Lifr
Procr
Row z-score
2
1
0
-1
D

**Figure 2.4. Isolation of Lifr$^+$ and Procr$^+$ stromal cell populations from dystrophic muscle.**

(A) Schematic of stromal cell sorting strategy used for bulk RNA sequencing analysis.

(B) Representative plots showing isolation of Lifr$^+$ and Procr$^+$ from MΦ cKO mice.

(C) Heatmap of z-scores generated from bulk RNAseq expression levels of key cluster markers in FAPs, Lifr$^+$, and Procr$^+$ cells isolated from skeletal muscle of control mice (n=3).

(D) RNA velocity plots of stromal cell subtypes from both MΦ cKO and control skeletal muscle.


Macrophage
Ligand activity
Stromal cell
Predicted target genes
Pearson
Prioritized ligands
Tgfb1
Adam17
Pik3cb
Il1b
Itgb7
Sema4d
Gas6
Yars
Nectin1
Itgam
Cxcl16
Sell
Ccl2
Itga4
C3
Spp1
Tnf
Itgb2
Osm
Copa
Pearson correlation coefficient
target gene prediction ability)
0.13 0.14 0.145 0.15 0.155
Regulatory potential
0.00 0.01 0.02

**Figure 2.5. Nichetnet analysis reveals TGFβ1 and Spp1 as critical ligands that regulate novel stromal cell target gene expression.**

Heatmap of ranked ligand-target gene regulatory potential shows cell-cell interactions between predicted ligands from macrophages with most likely regulated target genes that are differentially expressed in the novel stromal cell population from MΦ cKO and control as a reference.

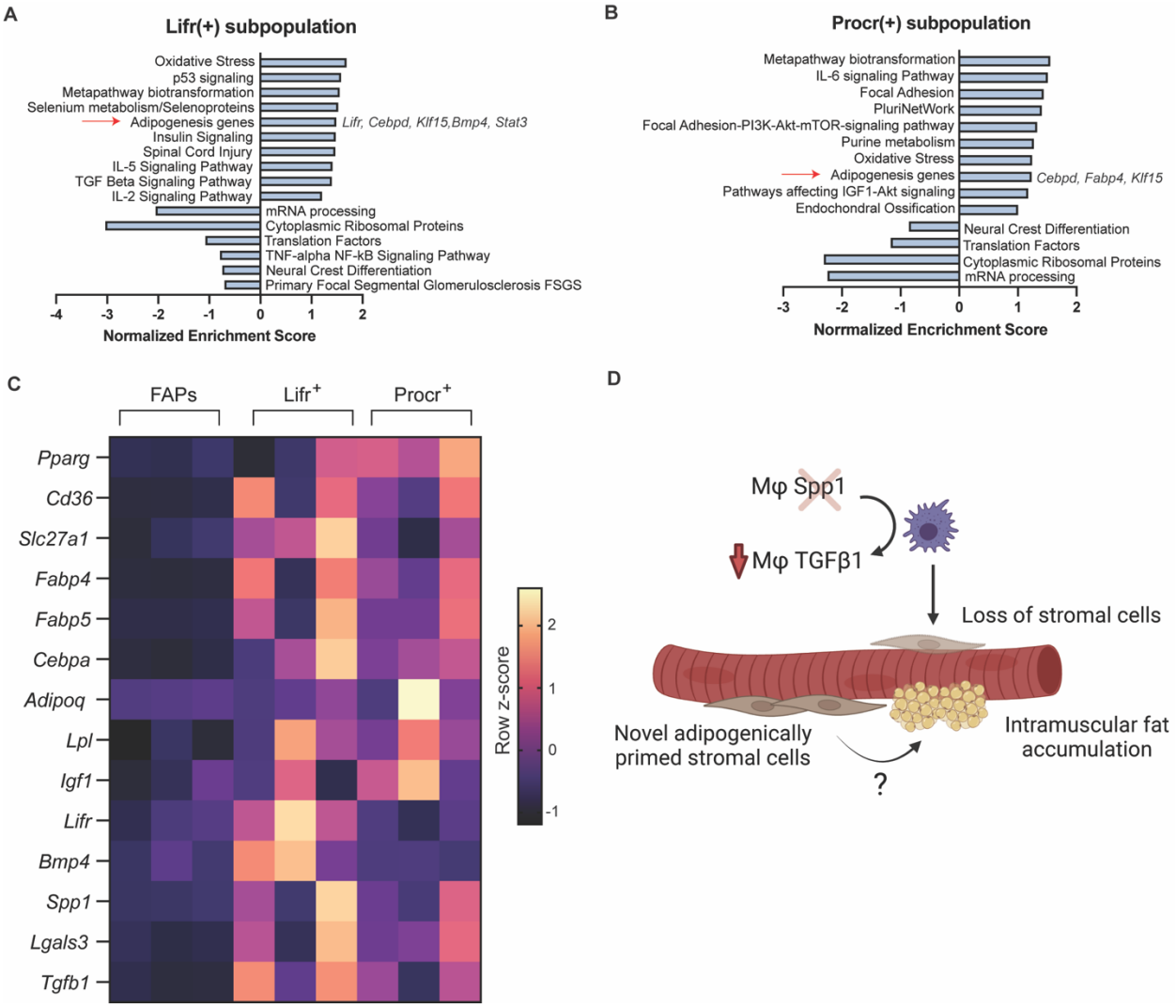
A
Lifr(+) subpopulation
Oxidative Stress
p53 signaling
Metapathway biotransformation
Selenium metabolism/Selenoproteins
Adipogenesis genes
Lifr, Cebpd, Klf15,Bmp4, Stat3
Insulin Signaling
Spinal Cord Injury
IL-5 Signaling Pathway
TGF Beta Signaling Pathway
IL-2 Signaling Pathway
mRNA processing
Cytoplasmic Ribosomal Proteins
Translation Factors
TNF-alpha NF-kB Signaling Pathway
Neural Crest Differentiation
Primary Focal Segmental Glomerulosclerosis FSGS
-4 -3 -2 -1 0 1 2
Normalized Enrichment Score
B
Procr(+) subpopulation
Metapathway biotransformation
IL-6 signaling Pathway
Focal Adhesion
PluriNetWork
Focal Adhesion-PI3K-Akt-mTOR-signaling pathway
Purine metabolism
Oxidative Stress
Adipogenesis genes
Cebpd, Fabp4, Klf15
Pathways affecting IGF1-Akt signaling
Endochondral Ossification
Neural Crest Differentiation
Translation Factors
Cytoplasmic Ribosomal Proteins
mRNA processing
-3 -2 -1 0 1 2
Norrmalized Encrichment Score
C
FAPs
Lifr+
Procr+
Pparg
Cd36
Slc27a1
Fabp4
Fabp5
Cebpa
Adipoq
Lpl
Igf1
Lifr
Bmp4
Spp1
Lgals3
Tgfb1
Row z-score
2
1
0
-1
D
Mφ Spp1
Mφ TGFβ1
Loss of stromal cells
Novel adipogenically primed stromal cells
Intramuscular fat accumulation
?

**Figure 2.6. Enrichment of adipogenesis genes in Lifr$^+$ and Procr$^+$ stromal cell populations.**

(A,B) Gene set enrichment analysis of significant differentially expressed genes in Lifr$^+$, and Procr$^+$ subpopulations from single cell RNAseq data.

(E) Z-score heatmap of bulk RNAseq expression levels of adipogenesis and TGFB1 related genes in FAPs, Lifr$^+$, and Procr$^+$ cells isolated from skeletal muscle of control mice (n=3).

(F) Schematic of conclusions.

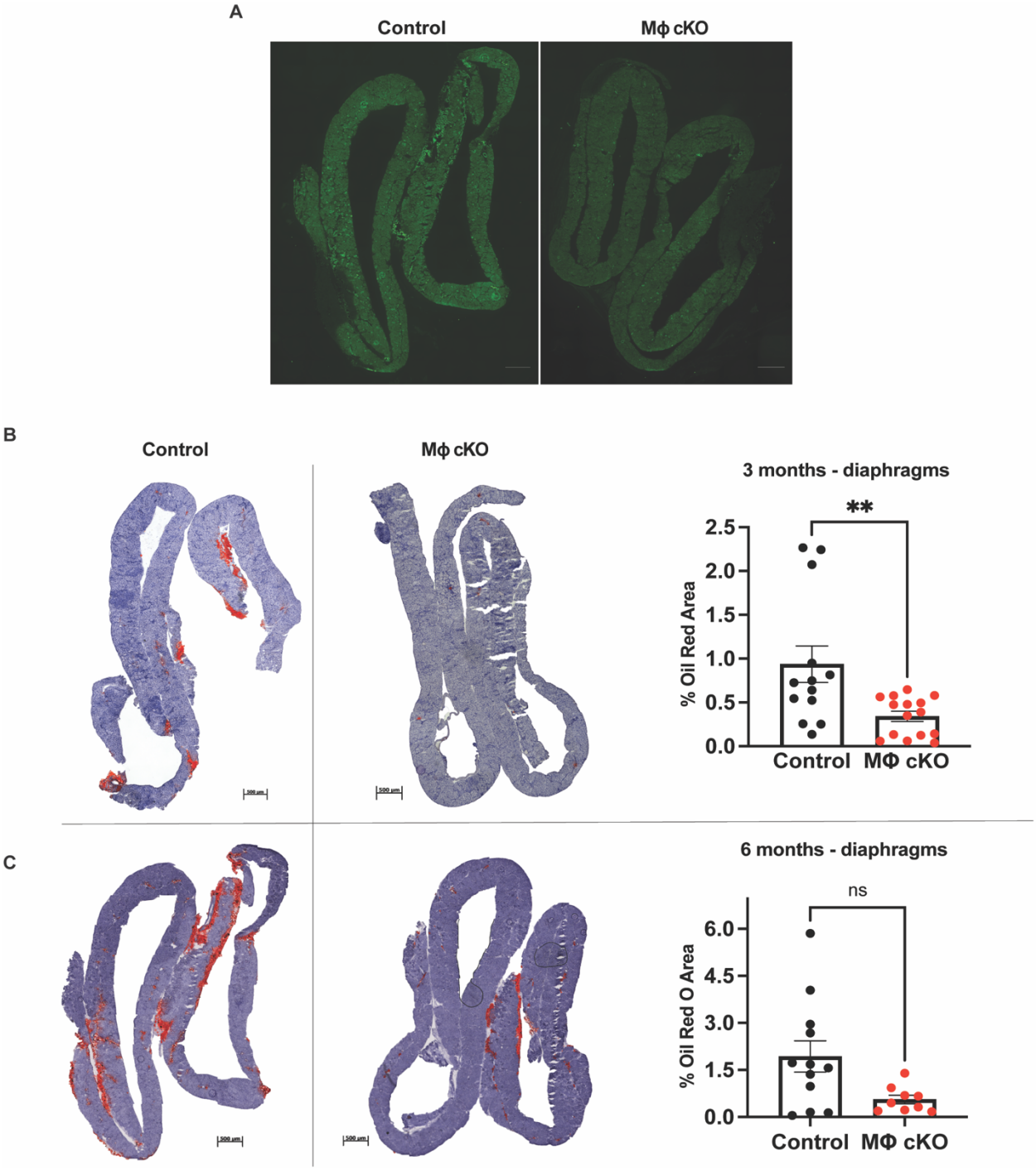
A
Control
Mϕ cKO
B
Control
Mϕ cKO
3 months - diaphragms
**
% Oil Red Area
2.5
2.0
1.5
1.0
0.5
0.0
Control
MΦ cKO
C
6 months - diaphragms
ns
% Oil Red O Area
6.0
4.5
3.0
1.5
0.0
Control
MΦ cKO

**Figure 2.7. Ablation of macrophage-derived Spp1 regulates intramuscular fat accumulation.**

(A) Immunofluorescent staining of perilipin in 6-month-old control and MΦ cKO diaphragms. Scale bar = 500um

(B,C) Quantification of percentage of Oil Red O area normalized to cross-sectional area in 3-month old diaphragms (top) and 6-month old diaphragms (bottom) from control (black) and MΦ cKO (red) mice. *P < 0.05 and ns > 0.05 using Mann-Whitney t-test.

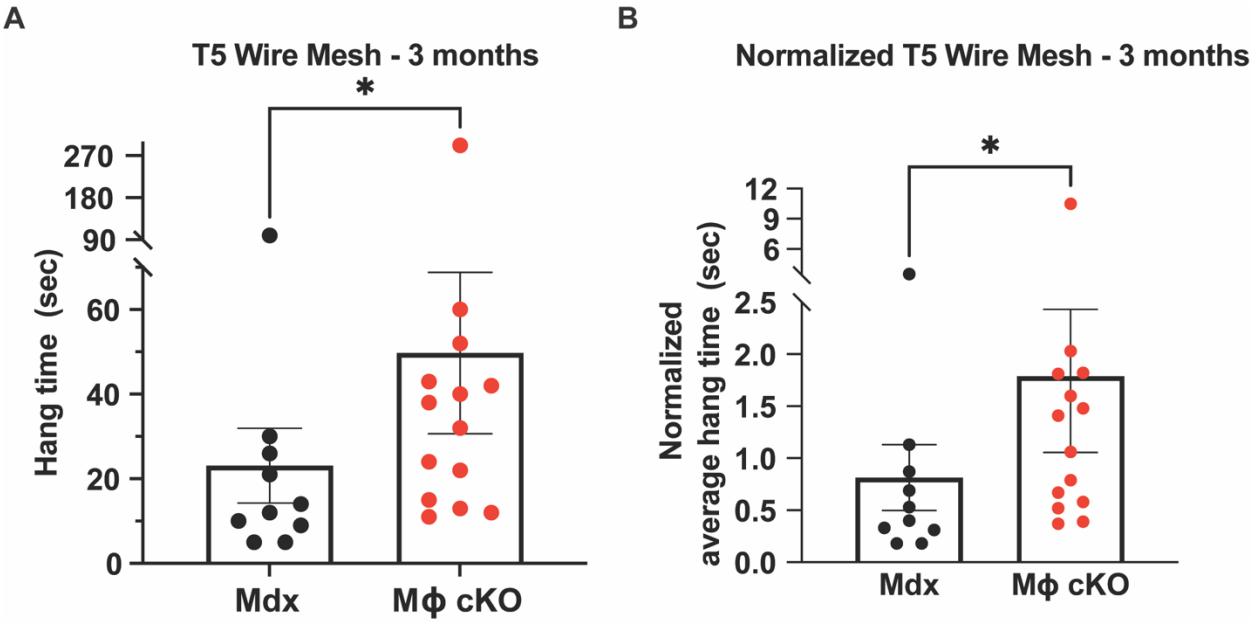
A
T5 Wire Mesh - 3 months
*
270
180
90
60
40
20
0
Hang time (sec)
Mdx
Mϕ cKO
B
Normalized T5 Wire Mesh - 3 months
*
12
9
6
2.5
2.0
1.5
1.0
0.5
0.0
Normalized average hang time (sec)
Mdx
Mϕ cKO

**Figure 2.8. Improved hang time endurance with ablation of macrophage derived Spp1 compared to control.**

(A) Average hang time of MΦ cKO (n=14) and control (n=10) mice on the fifth of five trials. *P=0.0318 determined by unpaired Mann-Whitney t-test.

(B) Average hang time of MΦ cKO (n=14) and control (n=10) mice on the fifth of five trials normalized to weight (g) of each mouse. *P=0.0472 determined by unpaired Mann-Whitney t-test.

# CHAPTER 3 – Effect of muscle stem cell derived Spp1 on the dystrophic muscle niche


## ABSTRACT

Duchenne muscular dystrophy (DMD) is a progressive muscle wasting disorder and is one of the most common genetically inherited diseases of childhood. DMD is caused by mutations in the *DMD* gene, which encodes for dystrophin protein wherein chronic cycles of degeneration and regeneration lead to repeated myofiber regeneration and necrosis, ultimately leading to failed regeneration in part as a result of overactivated muscle stem cells. Our previous work showed that osteopontin (SPP1) is a critical regulator of DMD disease progression[18,34]. Global knockout of *Spp1* in dystrophic mice (*Spp1* KO) showed a shift in macrophage polarization towards a pro-regenerative macrophage phenotype and an overall improvement in muscle regeneration and muscle function. SPP1 is expressed by a variety of cells within the muscle niche and can be post-translationally modified in many ways that could have differential effects on target cells. It is currently unknown how cell-specific sources of SPP1 influence cellular dynamics in dystrophic muscle. In this study we used single cell transcriptomics to elucidate how muscle stem cell (MuSC) derived SPP1 impacts cell-cell interactions in *mdx* mice. Here, we show that loss of MuSC specific *Spp1* has an autocrine effect on MuSC phenotype that promotes stemness and mitigates a fibrotic and inflammatory stem cell state. In MuSC cKO muscles, endothelial cells have a pro-angiogenic and anti-inflammatory phenotype compared to mdx controls. Additionally, macrophage polarization is shifted towards an M2:M1 ratio, suggesting that MuSC-derived Spp1 has an autocrine effect on macrophage phenotypes. This study provides evidence that MuSC Spp1 is a critical regulator of the interstitial muscle microenvironment, specifically via a MuSC-EC axis, which impacts macrophage phenotypes.

## INTRODUCTION

Duchenne muscular dystrophy (DMD) is a progressive muscle wasting disease that affects approximately 1 in 4000 male births each year[1]. DMD is an X-linked recessive disorder that is caused by mutations in the *DMD* gene that encodes for the dystrophin protein. Dystrophin is an important sarcolemmal molecular shock absorber that protects myofibers from contraction and injury-induced mechanical stress[2]. Lack of functional dystrophin expression causes myofiber membrane fragility leading to chronic cycles of muscle degeneration and regeneration.

In healthy non-injured muscle, $Pax7^+$ muscle stem cells (MuSCs) reside in the periphery of myofibers in a quiescent state[57]. Mechanical injury causes the release of cues from the microenvironment that drive MuSC activation setting off a carefully orchestrated migration of MuSCs out of their niche to the damaged area where subsequent cell cycle entry and proliferation occurs[57]. Additional factors from the microenvironment promote these myoblasts towards myogenic differentiation leading to myoblast fusion, myotube maturation and regeneration of mature myofibers[57]. In DMD, MuSCs have intrinsic phenotypic defects due to loss of dystrophin and can be extrinsically reprogrammed by aberrant inflammation and fibrosis accumulation that leads to MuSC exhaustion and ultimately failed regeneration[58].

MuSC have also been shown to play a wider role in the muscle microenvironment as they come into close contact with other interstitial cells like stromal cells, endothelial cells and immune cells[59]. MuSCs and myoblasts, in particular, are intimately associated with the muscle microvasculature and thus endothelial cells (ECs) that line these vessels[60–62]. This close proximity between MuSCs and endothelial cells facilitates MuSC quiescence and has been shown to impact immune cell recruitment[60–62]. This makes sense as ECs are in constant contact with immune cells like monocytes and macrophages and are important regulators of tissue inflammation.

Osteopontin (SPP1) is encoded by the *Spp1* gene and is one of the most highly upregulated transcripts in DMD. Our lab previously identified SPP1 as important immunomodulator that impacts fibrosis and muscle regeneration in the *mdx* mouse model of DMD[18,19,34]. In these studies, *mdx* mice with global ablation of *Spp1* showed an improved dystrophic phenotype, including increased muscle strength and regenerating myofibers[18]. Isolated F4/80(+) macrophages from SPP1 null mdx mice showed a shift in macrophage polarization towards an M2-like state and expressed higher transcript levels of pro-regenerative factors such as *Igf1*, *Lif* and *uPA*[34]. This pro-regenerative immune profile was correlated with increased muscle mass, increased myofiber cross-sectional area and improved muscle strength. These findings suggest that SPP1 plays a critical role in establishing a pro-regenerative microenvironment that supports proper muscle regeneration and repair.

SPP1 is matricellular protein that binds to a variety of receptors and other proteins such as integrins, CD44, and heparin[21]. It is expressed by a variety of cell types within the skeletal muscle niche such as immune cells, stromal cells, muscle fibers, endothelial cells and muscle stem cells[15,18,19,21,34]. Additionally, SPP1 can be post-translationally modified by phosphorylation, glycosylation, transglutamination, and cleaved by thrombin and metalloproteases, which may be determined in a cell-specific manner[15]. Due to this complexity, it is not understood how cell specific sources of SPP1 impact its effect on different target cells.

In this study, we elucidate how MuSC derived *Spp1* impacts cell-cell interactions in dystrophic muscle. We show by scRNAseq analysis that conditional ablation of *Spp1* in Pax7(+) cells (MuSC cKO) in mice on the *mdx* background results in an increased proportion of endothelial cells (ECs) and macrophage populations. We show that ECs in MuSC cKO significantly upregulate markers associated with angiogenesis and an anti-inflammatory response. Overall, our data suggests that MuSC specific *Spp1* has a localized effect on the interstitial niche, specifically acting on MuSCs, ECs in the vasculature of dystrophic muscle and ultimately the inflammatory microenvironment.

## MATERIALS AND METHODS

### *Animal husbandry*

Guidelines from the Animal Research Committee at UCLA were followed in the handling and breeding of all mice. Protocols for the care and use of animals were approved by the UCLA Office of Protection of Research Subjects.

### *Generation of Spp1 conditional knockout targeting vector*

The Spp1 region of accession #NT_109320.5 (28,332,597-28,344,133) was cloned into pBlueScript II SK(+) and inserted into the ApaI-EcoRV site. Loxp sites were inserted after exon 1 and before exon 4 of the *Spp1* locus to engineer removal of exons 2 and 3 and generate a premature stop codon.

### *Generation of Spp1 floxed dystrophic mice*

*Spp1 floxed* mice were generated by Mouse Biology Program at University of California, Davis. Targeting vector for floxed *Spp1* was electroporated into ES cells of C57BL/6N strain. Neomycin resistant cells were selected and microinjected into blastcysts of Balb/C strain. Mice with germline transmission were bred with FLP mice (C57BL/6N-Tg(CAG-Flpo)1Afst/Mmucd, provided from Mutated Mouse Resource & Research Center at University of California, Davis). Pups in which neomycin gene was excised were selected and bred. *Spp1* floxed mice were crossed to C57BL/10ScSn-Dmd$^{mdx}$/J (Jax #001801) mice were obtained by The Jackson Laboratories.

### *Crossing of Spp1 floxed mice with tissue-specific Cre-mdx mice*

Pax7$^{creER}$ (B6.Cg-Pax7$^{tm1(cre/ERT2)Gaka}$/J) for muscle stem cell-specific Cre was obtained from The Jackson Laboratories and crossed to *Spp1* floxed *mdx* mice.

*PCR for genotyping myeloid-specific Spp1 conditional knockout mice*

PCR genotyping of Pax7$^{creER}$ mice used the following primers: (Pax7$^{creER}$ mutant: 5'-CAA AAG ACG GCA ATA TGG TG-3'; Pax7$^{creER}$ common: 5'- GCT GCT GTT GAT TAC CTG GC-3'; Pax7 WT: 5'- CTG CAC TGA GAC AGG ACC G-3'). PCR for the floxed *Spp1* allele used the following primers: (Forward: 5'- GGA CCT TGA GTG ACT GGT TCT-3'; Reverse: 5'- TGG ACC TGA ACT CTG TGT GC-3')

*Cell isolation for single-cell RNAseq*

Mice were sacrificed and muscles from arms and hindlimbs (triceps, quadriceps, tibialis anterior, gastrocnemius) and diaphragm were pooled into a Petri dish containing sterile PBS (with $Ca^{2+}$, $Mg^{2+}$) for weighing. Muscles were washed in PBS (with $Ca^{2+}$, $Mg^{2+}$) and then minced in a 1:5 (weigh:volume) solution of 6mg/mL collagenase type 2 (Worthington Biochemical Corp.). To further digest the tissue, we transferred the tissue and collagenase solution to a 50mL conical tube in which we added a 1/1000 volume of DNAse I (final 20kunitz/mL) and placed at 37°C. Once the tissue was digested, the mixture was filtered through a 70um nylon filter and was washed with $Ca^{2+}$, $Mg^{2+}$-free PBS making sure not to add more than 1g muscle per tube. Cells were pelleted by centrifugation at (330xg) for 5 minutes. After discarding the supernatant and breaking up the pellet with 5mL of $Ca^{2+}$, $Mg^{2+}$-free PBS, we filled the conical tube with $Ca^{2+}$, $Mg^{2+}$-free PBS and centrifuged again for 10 minutes. We used a Cell Debris Removal kit (Miltenyi) and centrifuged at (300xg**)** at 4°C. After removing the PBS and interphase (cell debris) layers, cells were washed with $Ca^{2+}$, $Mg^{2+}$-free PBS and centrifuged again at (3000xg) at 4°C. Cells were resuspended in ACK lysis buffer (Lonza) to lyse red blood cells and centrifuged at

(300xg) at 4°C for 10 minutes. Pellet was resuspended in $Ca^{2+}$, $Mg^{2+}$-free PBS and cells were filtered with a 40um nylon filter and washed with additional $Ca^{2+}$, $Mg^{2+}$-free PBS. After centrifugation (300xg) at 4°C, we used a Dead Cell Removal Kit. The purified cell solution was centrifuged at (300xg) at 4°C. We discarded the supernatant and resuspended the cell pellet in a 0.04% BSA solution. To count cells, a small sample volume was mixed 1:1 with 0.4% Trypan blue solution and counted using a hemocytometer.

*scRNAseq library construction, sequencing and data analysis*

scRNAseq was conducted on cells isolated from murine skeletal muscle (pooled from three mice per genotype). Libraries were constructed using the Chromium Single Cell 3' Reagent Kits v3 (10X Genomics) at the UCLA Technology Center for Genomics & Bioinformatics (TCGB). cDNA libraries were sequenced on the NextSeq500 High Output platform using to achieve approximately 20,000 reads/cell. Sequencing reads were processed using the 10X Genomics Cell Ranger (Seurat version 3.0) was used.

*Flow sorting and cytometry*

Endothelial cells and muscle stem cells from MuSC cKO and control mice were isolated, dissociated and minced in 500U/mL collagenase II (Worthington) and incubated at 37°C and slowly rocked for 30 minutes. Muscles were washed with DPBS(-/-) + 10% PBS and centrifugated at (600xg). Minced muscles were further dissociated in a solution consisting of 1.5U/mL collagenase D (Roche) and 2.4U/mL dispase (Worthington) and incubated and slowly rocked for 45 minutes. Dissociated cells were then filtered using 40um cell strainers. Zombie-APC-Cy7 (1:500, Biolegend) was used for live cell discrimination and treated with Fc block (CD16/32) (1:50, Biolegend). The cells were then stained using the following primary antibodies: CD45-Pacific Blue (1:1000, Biolegend), SCA1-Pacific Blue (1:500, Biolegend), ITGA7-PE (1:100, R&D), CD31-APC (1:200, BD Biosciences) for 45 minutes at 4°C. CD31(+) cells

(endothelial cells) and ITGA7(+) cells (muscle stem cells) were isolated using a FACSAria II sorter (BD Biosciences) into DMEM media.

*Bulk RNAseq*

Total RNA was isolated using the Zymo Quick RNA Micro Prep Kit. RNA libraries were prepared by the UCLA TCGB Core and sequencing was performed on NextSeq500 Mid Output.

*Muscle dissection, freezing and histology*

Muscles were dissected, covered with Tissue-Tek OCT mounting media and frozen in liquid nitrogen-cooled isopentane. 10um sections were cut on a (cryostat name here) and stored at -20°C.

## RESULTS

*Generation of Spp1 conditional knock out*

To assess the effect of MuSC derived *Spp1* on the dystrophic niche, we generated a MuSC *Spp1* conditional knockout mouse line using the inducible Pax7ER$^{T2}$ driver as Pax7 is critical marker of MuSCs. Pax7ER$^{T2}$ mice were crossed to *Spp1 fl/fl* mice congenic to the *mdx* BL/10 background (hereto after called MuSC cKO). Treatment with two weeks of tamoxifen chow induced a premature stop codon at the *Spp1* locus leading to knockdown of Spp1 expression specifically in Pax7$^{+}$ MuSCs. Additionally, we crossed these mice to Ai6 reporter strain that expresses ZsGreen at the ROSA locus to specifically label Pax7$^{+}$ cells following Cre-mediated recombination.

*Effect of MuSC derived Spp1 on cellular frequencies and phenotypes in the dystrophic niche*

To determine how MuSC derived *Spp1* impacts cellular profiles within dystrophic muscle, we isolated cells from limb and diaphragm muscle from 3-month-old MuSC cKO and

control mice and scRNAseq libraries were generated using 10x Genomics. We analyzed 8,137 cells from MuSC cKO muscle and 17,817 cells from control muscle, which revealed 12 major cell types: stromal cells (Stromal, SC), immune and blood cell populations such as macrophages (Macs), T-cells (TC), B-cells (BC), neutrophils, (NP), NK cells (NK), erythrocytes (RBC), cycling leukocytes, and a variety of interstitial cells like endothelial cells (EC), Pax7(+) cells, nerve cells (NC) and smooth muscle cells (SMC) (**Figure 3.1A,B**). We further analyzed how these cellular profiles changed by genotype (**Figure 3.1C**) and found that there was a striking increase in the proportion of endothelial cells and macrophage populations from MuSC cKO muscle compared to control (**Figure 3.1C,D**). While immune cells are well known for expressing OPN, our lab has shown that it is also widely expressed throughout the muscle[18,19]. This data suggests that MuSC derived *Spp1* does impact the dystrophic muscle milleu.

*Autocrine regulation of Spp1 on MuSC phenotype*

To determine the effect of loss of *Spp1* in MuSCs, we conducted bulk RNAseq analysis from FACS isolated ZsGreen$^{+}$ cells, which specifically labels Pax7$^{+}$ cells, from 12-week-old MuSC cKO and control mice treated with two weeks of tamoxifen chow (**Figure 3.2A**). Analysis of significant DEGs showed an upregulation of markers associated with positively regulating stemness of Pax7$^{+}$ cells such as *Pax7*, *Pax3* and Notch downstream target genes such as *Heyl* and *Hey1* in MuSCs cKO compared to control (**Figure 3.2B**). Interestingly, we also see a decrease in a variety of fibrotic/extracellular matrix associated genes such as *Lox*, *Ctgf* and *Col1a1* (**Figure 3.2C**) and a decrease in inflammatory genes like *Ccl2* (**Figure 3.2D**). We validated these observations by RT-qPCR and showed an increase in the stemness marker *Myf5* and a corresponding decrease in ECM and inflammatory markers *Col1a1*, *Ctgf* and *Ccl2*, respectively, in MuSC cKO compared to control. This data suggests that loss of MuSC *Spp1* improves the overall MuSC phenotype such that they retain a more stem-like state and have a reduced pro-fibrotic and inflammatory profile.

Since the ZsGreen reporter marked any cell that expresses or had expressed $Pax7^+$ and may be retained in cells that have differentiated further, we used an alternative sorting strategy to more specifically assess the profile of MuSCs after loss of MuSC-derived *Spp1*. To do this, we used FACS to isolate $Lin^-$ ($CD45^-SCA1^-CD31^-$), $ITGA7^+$ cells from 13-week-old MuSC cKO and control nice and conducted bulk RNA sequencing (**Figure 3.3A**). Analysis of significant DEGs confirmed upregulation of genes like *Spry1*, *Notch1* and downstream regulators *Hey1* and *Heyl* that are positively associated with retaining MuSC stemness (**Figure 3.3B**). We also saw downregulation of active cell cycle markers such as *Mki67* and *Top2a* suggesting reduced MuSC activation. While we saw upregulation of various collagen genes, we saw downregulation of key regulators of fibrosis such as *Ltbp4* and *Lox*. Additionally, we confirmed reduction of inflammatory genes like *Ccl2* and *Il1a*. Overall, these data provide evidence that MuSC derived Spp1 is an autocrine regulator of MuSC phenotype that maintains a stem-like, homeostatic state.

*MuSC derived Spp1 impacts endothelial cell heterogeneity and transcriptional profile*

Studies have shown that the close proximity of MuSCs to capillaries and other vessels allows that facilitates reciprocal MuSC-EC interactions[61,62]. To better understand the impact of MuSC Spp1 on endothelial cells, we conducted further subcluster analysis of ECs. A recent study characterized a variety of endothelial cell subpopulations within normal, dystrophic and severely dystrophic muscle[63]. Using these markers, we identified eight EC subtypes including two capillary EC clusters which are part of the microvasculature (clusters 0 and 1), pericytes that provide structural support to vessels (cluster 2), two arterial clusters indicative of large vessel subtypes (clusters 3 and 5), activated ECs marked by *Spp1* expression (cluster 4), venous ECs (cluster 5) and lymphatic ECs (cluster 6) (**Figure 3.4A**). While we saw the overall proportion of ECs increased with ablation of MuSC derived *Spp1* (Figure 1D), we only saw an increase in specific EC subtypes (**Figure 3.4B,C**). Capillary EC1, pericytes and arterial EC2

clusters expanded while there was a reduction in arterial EC1. Next, we wanted to understand how MuSC derived Spp1 impacted the transcriptional profile of endothelial cells. Interestingly, volcano plot of significant DEGs showed upregulation of *Cxcl12*, a cytokine associated with chemotaxis, macrophage polarization and neovascularization[64,65] (**Figure 3.4D, top**). Many of the clusters that expanded in the MuSC cKO show high expression of *Cxcl12* while those that contracted such as Arterial EC1 show little to no *Cxcl12* expression (**Figure 3.4D, bottom**). This data suggests that MuSC derived Spp1 may not only impact EC frequencies, but EC transcriptional profile as well.

We isolated endothelial cells ($CD45^-SCA1^-ITGA7^-CD31^+$) using FACS and conducted bulk RNAseq analysis to determine if MuSC-specific Spp1 alters endothelial cell phenotype. Metascape analysis of significant DEGs showed upregulation of ERK signaling and vascular processes suggesting maintenance of endothelial homeostasis[66] (**Supplemental Figure 3.1**). Genes associated with leukocyte migration and regulation of mononuclear cell migration were downregulated. Analysis of significant DEGs showed that ECs had increased expression of anti-inflammatory and pro-angiogenic markers and reduced expression of inhibitors of angiogenesis, EC activation and pro-inflammatory markers in MuSC cKO mice compared to control (**Figure 3.4F,G**). Interestingly, while the proportion of activated ECs (cluster 4) did not change by genotype the expression of markers associate with EC activation was downregulated including *Spp1* and *Sox4* (**Figure 3.4E**). This data suggests that MuSC Spp1 may play a role in maintaining endothelial cells in a homeostatic, anti-inflammatory state and has a paracrine effect on EC *Spp1* expression.

*MuSC derived Spp1 impacts macrophage polarization*

Endothelial cells come into close proximity with immune cells. EC-immune cell crosstalk plays an important role in the inflammatory microenvironment. In addition to the EC clusters expansion, we see an increase in the proportion of macrophage populations from MuSC cKO

mice (**Figure 3.1D**). We characterized four transcriptionally distinct macrophage subpopulations and a dendritic cell population (**Figure 3.5A,B**). We observed a striking decrease in the M1-like macrophage subtype and a correlated increase in M2c-like macrophages (**Figure 3.5A**) in MuSC KO compared to control, which corresponds with the changes in macrophage subtypes in the global Spp1 KO[34]. We saw a 2.5-fold increase in the M2:M1 ratio indicating a shift in macrophage polarization when MuSC derived *Spp1* was ablated (**Figure 3.5C**). However, volcano plot of significant DEGs showed that *Spp1* is highly upregulated in MuSC cKO macrophage cells compared to control (**Figure 3.5D**). While the mechanism remains to be elucidated, this data suggests that MuSC derived Spp1 plays either a direct or indirect role in macrophage polarization, but does not alter macrophage Spp1 expression.

## DISCUSSION

In this study we conducted an unbiased scRNAseq transcriptomic analysis of dystrophic muscle to better understand the impact of MuSC-specific Spp1 on cell-cell interactions. We found that $Pax7^+$ cells were more stem cell-like and had a reduced fibrotic and inflammatory transcriptional profile with ablation of MuSC specific *Spp1*. We provide evidence that MuSC Spp1 has a paracrine effect on ECs such that there was an expansion of various endothelial cell subpopulations such as capillary ECs, pericytes and arterial ECs in MuSC cKO mice compared to control. We also observed an effect on the overall EC transcriptional profile as ECs from MuSC cKO mice were enriched in pro-angiogenic, anti-inflammatory markers and had a reduction in pro-inflammatory markers and genes associated with EC activation compared to control. Additionally, we saw a marked reduction in macrophage polarization away from an M1-like phenotype and towards an M2c-like phenotype, which we hypothesize could be influenced by the EC microenvironment.

Dystrophic muscle is known to highly upregulate osteopontin levels compared to WT, non-dystrophic muscle[18]. We previously showed that loss of global Spp1 in dystrophic mice

showed improved muscle regeneration and strength[18,34]. While immune cells are known to be the leading source of Spp1 in the muscle niche[67], skeletal muscle myoblasts have been shown to express Spp1 *in vivo*, in primary cultures and in the myogenic cell line, C2C12[68,69]. Our study is the first to our knowledge to uncover that MuSC derived *Spp1* has an autocrine negative regulatory effect on the stem-like transcriptional profile of MuSCs.

Maintaining MuSCs in a reversible stem cell, quiescent state after injury is important for conserving the regenerative capacity of these cells and general muscle homeostasis. While many studies have shown that extrinsic cues are important for pushing MuSCs towards activation/differentiation after injury, intrinsic cues are just as important[70]. Notch signaling, specifically Notch1, promotes a regenerative stem cell pool and is a positive regulator of Pax7 expression[71,72]. Spry1 was found to mark quiescent Pax7$^{+}$ cells but not cycling MuSCs and differentiating MuSCs in injured and noninjured muscle suggesting that it is a marker of quiescence[73]. Additionally, Wnt4 signaling regulates the cytoskeleton and mechano-properties of MuSCs via a RhoA-YAP pathway, which keeps maintains the MuSC in a rounded, quiescent state[74]. The significant upregulation of key markers such as *Spry1*, *Notch1* and its downstream targets *Hey1*/*Heyl* and *Wnt4* in ITGA7$^{+}$ MuSCs from MuSC cKO mice provide evidence that these cells are in a more intrinsically quiescent state. This is particularly critical for DMD as the overactivation of MuSCs due to chronic injury and inflammation leads to muscle exhaustion and failed regeneration[57,75].

Furthermore, we observed that loss of MuSC derived *Spp1* also an autocrine effect on expression of fibrotic/ECM and inflammatory markers, which may impact the cells in the local microenvironment. Studies have shown that over half of the MuSCs are in close proximity or in direct contact with capillaries[61,62] and directed crosstalk from MuSCs to ECs can recruit capillary ECs altering microvasculature patterning in hindlimb muscle[62]. We hypothesize that MuSC derived Spp1 may act as a regulator the of the satellite cell juxtavascular niche. The overall proportion of ECs from MuSC cKO mice expand compared to control, specifically subtypes such

as capillary EC1, pericytes and arterial EC2. We observed that MuSC cKO ECs were in a more anti-inflammatory, pro-angiogenic state and a reduced activated state compared to control. Notably, we see that *Sox4* is significantly downregulated in MuSC cKO ECs compared to control, a marker which has recently been shown to promote endothelial dysfunction via the TGFβ1 signaling in the context of atherosclerosis[76].

Interestingly, a recent study identified *Spp1* as a marker of activated ECs[63]. We observed that MuSC cKO ECs had significant downregulation of *Spp1* compared to control. This finding is significant as it suggests that MuSC derived Spp1 is having a local effect on Spp1 in cells in the surrounding microenvironment. There is evidence that DMD muscles are more poorly vascularized and have altered angiogenic potential[77], but our understanding of how endothelial dysfunction is impacted on a cellular level is limited. Future studies regarding MuSC Spp1 as a negative regulator of EC phenotype may be an important avenue for future stem cell therapies.

ECs create a selectively permeable barrier that maintains homeostasis in organs and tissues. In the cardiovascular field, it is well known that endothelial activation can prime the vasculature towards pathological disease such as in the case of atherosclerosis[78]. Mechanical and biochemical signals can greatly alter the state of ECs and push these cells towards an activated state that facilitates overactive recruitment and transmigration of immune cells into tissues[79–81]. We hypothesize that the altered phenotypic state of ECs, which can be regulated by MuSC-specific Spp1, could influence macrophage polarization. Whether the increased in M2:M1 ratio in of MuSC cKO muscle compared to control is due to reduced monocyte recruitment and infiltration or there is an EC-derived factor that promotes M2-like differentiation is yet to be determined. scRNAseq analysis showed that *Cxcl12* expression was increased in MuSC cKO ECs, which is associated with promoting macrophage polarization, but we could not confirm this by bulk RNAseq of isolated ECs. Lastly, we specifically see an increase in M2c-like cells, which

are the primary source of Spp1, and a concomitant significant upregulation of Spp1 in macrophages from MuSC cKO.

In conclusion, this study provides a deeper understanding of cell-specific SPP1 biology and its role in both autocrine and paracrine communication pathways in MuSC quiescence, endothelial dysfunction and immune regulation.

ACKNOWLEDGEMENTS

We thank Jane Wen, Diana Becerra, Jesus Perez and Bradley Smith for technical assistance. We thank the UCLA Technology Center for Genomics & Bioinformatics and the UCLA Jonsson Comprehensive Cancer Center Flow Cytometry Core, specifically Trent Su, Salem Haile and Iris Williams, for sequencing, access to equipment and analysis for this study. This work was supported in part by a Howard Hughes Medical Institute Gilliam Fellowship (GT11023) to R.A. and M.S., the UCLA Muscle Biology, Pathophysiology, and Therapeutics Training Program (NIH NIAMS T32 AR065972) to R.A., and NIH-NINDS R01NS117912, NIH-NIAMS P50 AR052646, DOD MD190060 (to M.S.), and NIH NINDS RO1 NS120060 (to S.V.).

# FIGURES

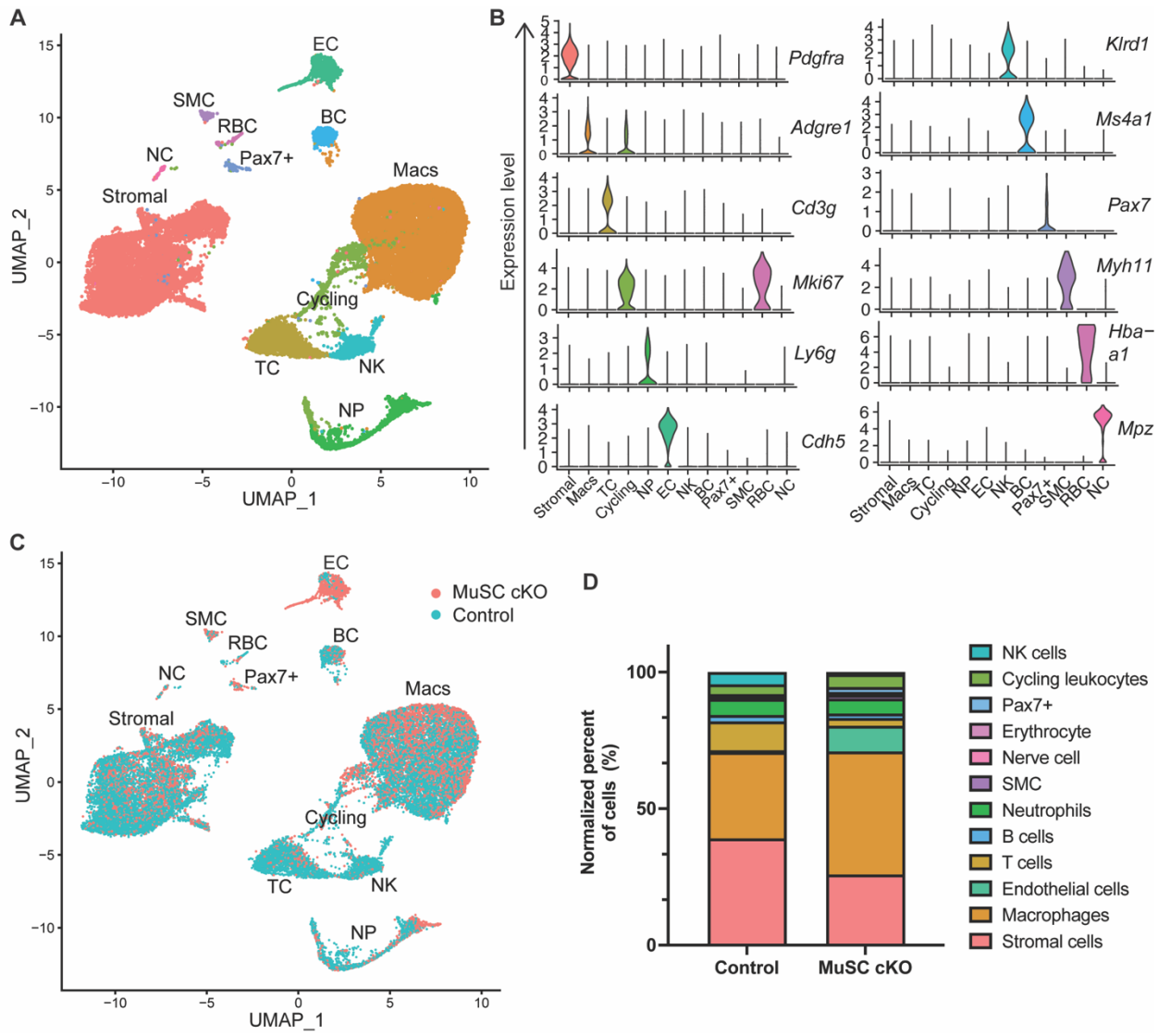
A
EC
SMC
RBC
BC
NC
Pax7+
Macs
Stromal
Cycling
TC
NK
NP
UMAP_2
UMAP_1
B
Expression level
Pdgfra
Adgre1
Cd3g
Mki67
Ly6g
Cdh5
Klrd1
Ms4a1
Pax7
Myh11
Hba−a1
Mpz
Stromal
Macs
TC
Cycling
NP
EC
NK
BC
Pax7+
SMC
RBC
NC
C
MuSC cKO
Control
D
Normalized percent of cells (%)
100
50
0
Control
MuSC cKO
NK cells
Cycling leukocytes
Pax7+
Erythrocyte
Nerve cell
SMC
Neutrophils
B cells
T cells
Endothelial cells
Macrophages
Stromal cells

**Figure 3.1. scRNAseq reveals MuSC Spp1 has a paracrine effect on endothelial cells and macrophages cellular frequencies.**

(A) UMAP plot shows unsupervised clustering of cells isolated from 12-week-old MuSC cKO and control skeletal muscle (n=3 per genotype).

(B) Violin plots of representative markers used in cell type annotation.

(C) UMAP plot depicting distribution of cells isolated from MuSC cKO (pink) and control (blue) skeletal muscle (n=3 per genotype).

(F) Proportion of each cell type (normalized to total cells) and how they change by genotype.

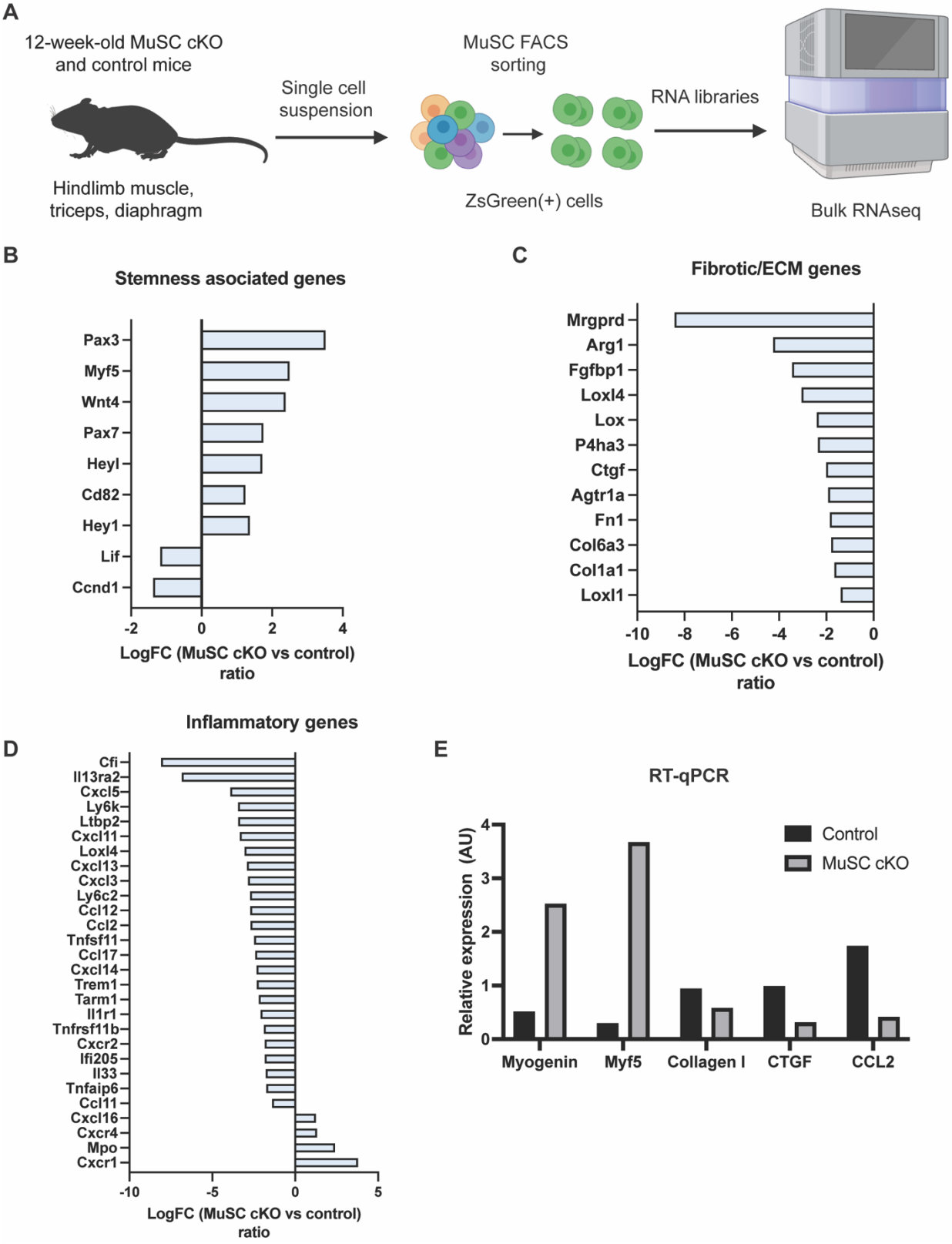
A
12-week-old MuSC cKO and control mice
Hindlimb muscle, triceps, diaphragm
Single cell suspension
MuSC FACS sorting
ZsGreen(+) cells
RNA libraries
Bulk RNAseq
B
Stemness asociated genes
Pax3
Myf5
Wnt4
Pax7
Heyl
Cd82
Hey1
Lif
Ccnd1
-2
0
2
4
LogFC (MuSC cKO vs control) ratio
C
Fibrotic/ECM genes
Mrgprd
Arg1
Fgfbp1
Loxl4
Lox
P4ha3
Ctgf
Agtr1a
Fn1
Col6a3
Col1a1
Loxl1
-10
-8
-6
-4
-2
0
LogFC (MuSC cKO vs control) ratio
D
Inflammatory genes
Cfi
Il13ra2
Cxcl5
Ly6k
Ltbp2
Cxcl11
Loxl4
Cxcl13
Cxcl3
Ly6c2
Ccl12
Ccl2
Tnfsf11
Ccl17
Cxcl14
Trem1
Tarm1
Il1r1
Tnfrsf11b
Cxcr2
Ifi205
Il33
Tnfaip6
Ccl11
Cxcl16
Cxcr4
Mpo
Cxcr1
-10
-5
0
5
LogFC (MuSC cKO vs control) ratio
E
RT-qPCR
Relative expression (AU)
0
1
2
3
4
Control
MuSC cKO
Myogenin
Myf5
Collagen I
CTGF
CCL2

**Figure 3.2. MuSC derived Spp1 has an autocrine effect on Pax7(+) cell phenotype.**

(A) Schematic of MuSC single cell isolation workflow to create RNA libraries for bulk RNA sequencing. Single cell homogenates from various skeletal muscles from 12-week old MuSC cKO (n=3) and control (n=3) mice that were treated with two weeks of tamoxifen were sorted to isolate cells $Pax7^{pos}$ cells labeled with ZsGreen fluorescent reporter.

(B) Log-fold change ratio of myogenic genes in MuSC cKO compared to control $ZsGreen^{pos}$ cells.

(C) Log-fold change ratio of inflammatory genes in MuSC cKO compared to control $ZsGreen^{pos}$ cells.

(D) Log-fold change ratio of fibrotic genes in MuSC cKO compared to control $ZsGreen^{pos}$ cells.

(E) RT-qPCR quantification of key myogenic, fibrotic and inflammatory markers from MuSC cKO (grey) and control (black) cells.

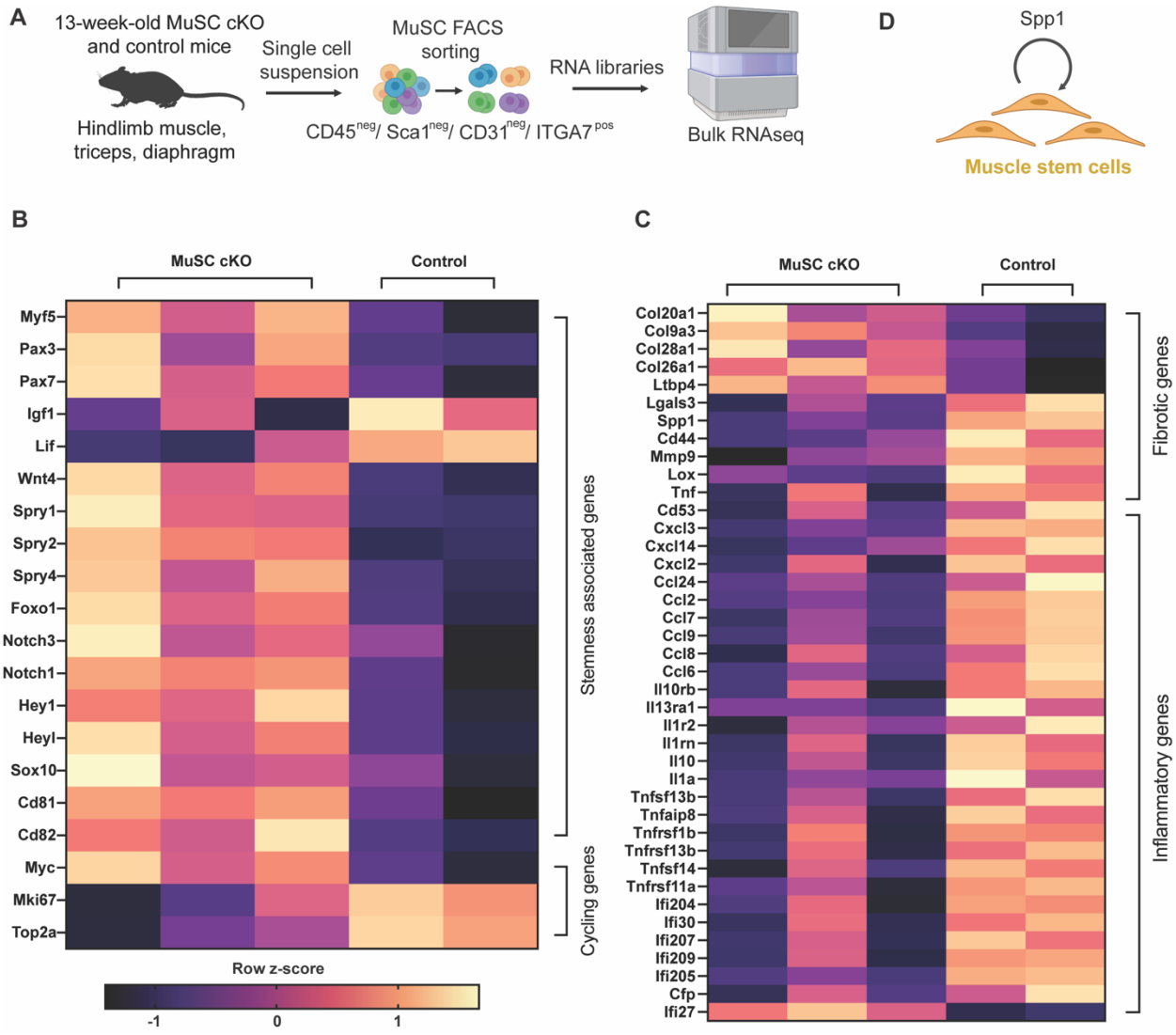
A
13-week-old MuSC cKO and control mice
Hindlimb muscle, triceps, diaphragm
Single cell suspension
MuSC FACS sorting
CD45neg/ Sca1neg/ CD31neg/ ITGA7pos
RNA libraries
Bulk RNAseq
D
Spp1
Muscle stem cells
B
MuSC cKO
Control
Myf5
Pax3
Pax7
Igf1
Lif
Wnt4
Spry1
Spry2
Spry4
Foxo1
Notch3
Notch1
Hey1
Heyl
Sox10
Cd81
Cd82
Myc
Mki67
Top2a
Stemness associated genes
Cycling genes
Row z-score
-1
0
1
C
MuSC cKO
Control
Col20a1
Col9a3
Col28a1
Col26a1
Ltbp4
Lgals3
Spp1
Cd44
Mmp9
Lox
Tnf
Cd53
Cxcl3
Cxcl14
Cxcl2
Ccl24
Ccl2
Ccl7
Ccl9
Ccl8
Ccl6
Il10rb
Il13ra1
Il1r2
Il1rn
Il10
Il1a
Tnfsf13b
Tnfaip8
Tnfrsf1b
Tnfrsf13b
Tnfsf14
Tnfrsf11a
Ifi204
Ifi30
Ifi207
Ifi209
Ifi205
Cfp
Ifi27
Fibrotic genes
Inflammatory genes

**Figure 3.3. MuSC derived Spp1 has an autocrine effect on muscle stem cell phenotype.**

(A) Schematic of MuSC single cell isolation workflow to create RNA libraries for bulk RNA sequencing. Single cell homogenates from various skeletal muscles from 13-week old MuSC cKO (n=3) and control (n=3) mice that were treated with two weeks of tamoxifen were sorted to isolate MuSCs that were $CD45^{neg}$/$SCA1^{neg}$/$CD31^{neg}$/$ITGA7^{pos}$.

(B) Z-score heatmap of muscle-specific, quiescence and cycling significant differentially expressed genes in cells isolated MuSC cKO and control mice.

(C) Z-score heatmap of fibrotic and inflammatory genes significant differentially expressed genes in cells isolated MuSC cKO and control mice.

(D) Schematic of autocrine regulation of Spp1 in MuSCs.

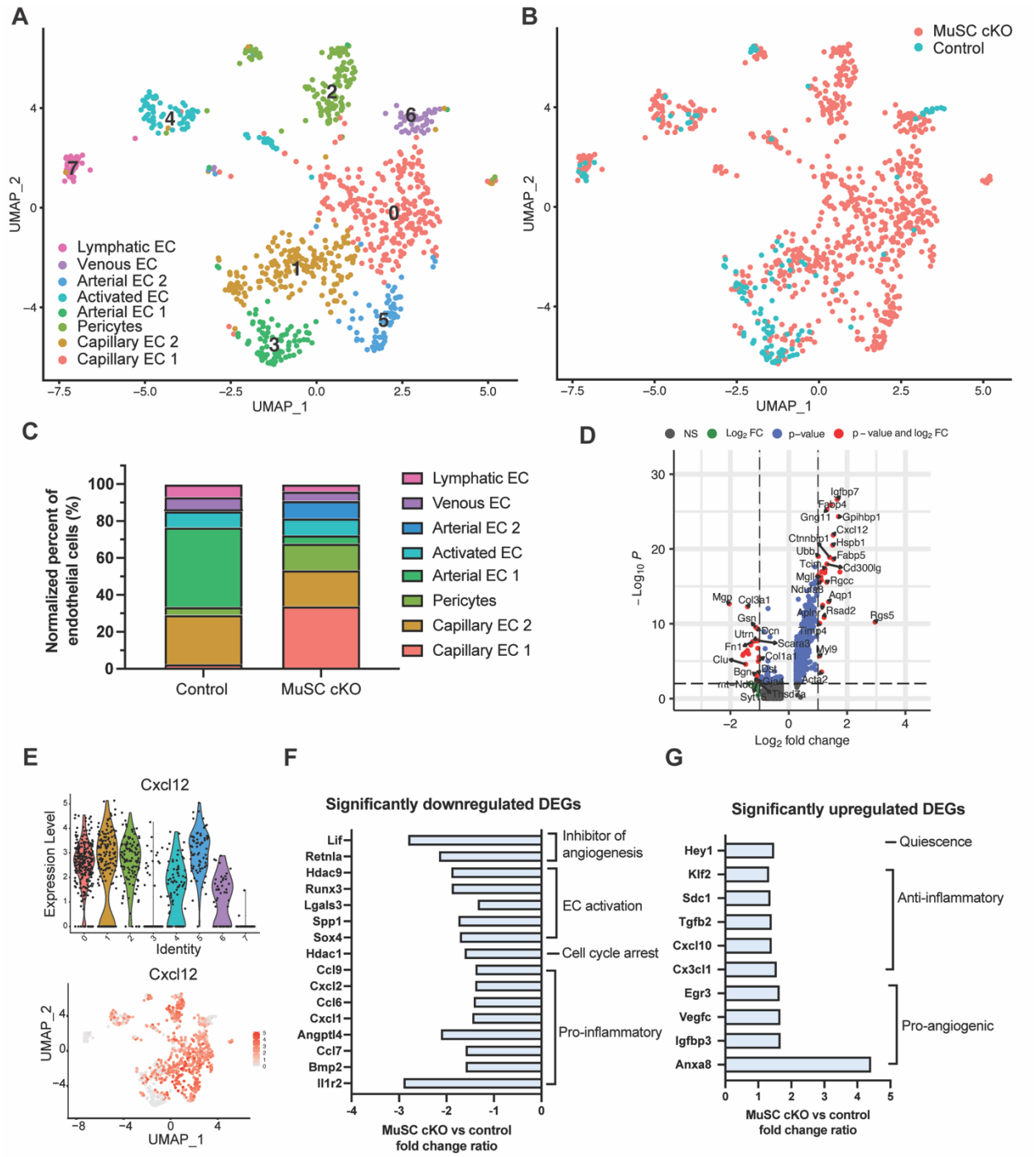
A
B
C
D
E
F
G
UMAP_1
UMAP_2
Lymphatic EC
Venous EC
Arterial EC 2
Activated EC
Arterial EC 1
Pericytes
Capillary EC 2
Capillary EC 1
MuSC cKO
Control
Normalized percent of endothelial cells (%)
Control
MuSC cKO
NS
Log2 FC
p–value
p – value and log2 FC
– Log10 P
Log2 fold change
Cxcl12
Expression Level
Identity
Significantly downregulated DEGs
Lif
Retnla
Hdac9
Runx3
Lgals3
Spp1
Sox4
Hdac1
Ccl9
Ccl2
Ccl6
Cxcl1
Angptl4
Ccl7
Bmp2
Il1r2
Inhibitor of angiogenesis
EC activation
Cell cycle arrest
Pro-inflammatory
MuSC cKO vs control fold change ratio
Significantly upregulated DEGs
Hey1
Klf2
Sdc1
Tgfb2
Cxcl10
Cx3cl1
Egr3
Vegfc
Igfbp3
Anxa8
Quiescence
Anti-inflammatory
Pro-angiogenic
MuSC cKO vs control fold change ratio

**Figure 3.4. EC subcluster analysis reveals EC heterogeneity is regulated by MuSC-derived Spp1.**

(A) UMAP plot shows unsupervised subclustering of endothelial cell subpopulations from MuSC cKO and control skeletal muscle.

(B) UMAP plot of EC subtype identity by genotype, MuSC cKO (pink) and control (blue).

(C) Proportion of each cell type (normalized to total stromal cells) by genotype.

(D) Violin plot of differentially expressed genes where $log_2$fold change < 1.0 and p-value in <0.01.

(E) Violin plot (left) and UMAP plot (right) of *Cxcl12* expression in each cluster.

(F) Bulk RNAseq fold change expression ratio of significantly downregulated genes from isolated endothelial cells from MuSC cKO vs control cells.

(G) Bulk RNAseq fold change expression ratio of significantly upregulated genes from isolated endothelial cells from MuSC cKO vs control cells.

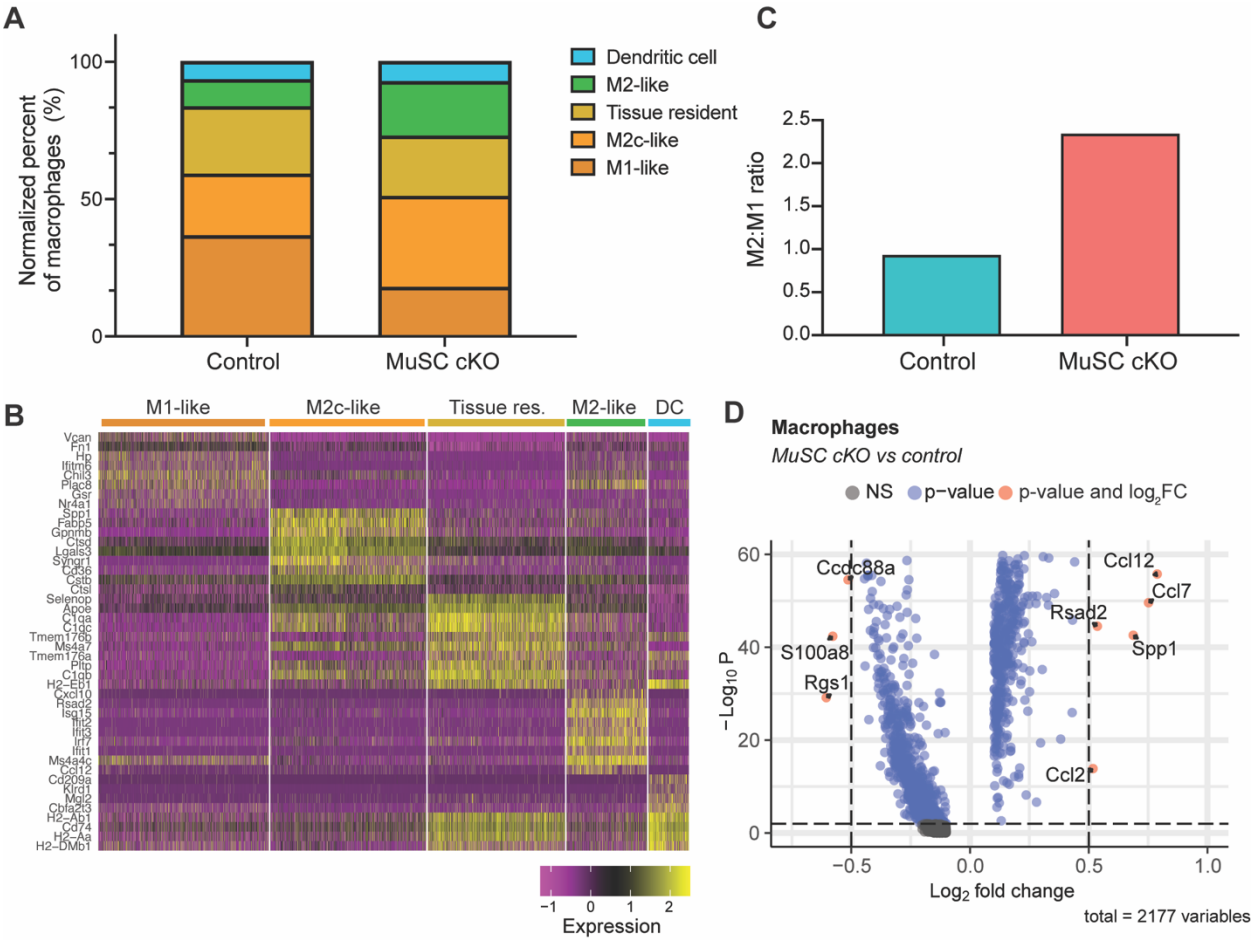
A
Normalized percent of macrophages (%)
100
50
0
Control
MuSC cKO
Dendritic cell
M2-like
Tissue resident
M2c-like
M1-like
C
M2:M1 ratio
2.5
2.0
1.5
1.0
0.5
0.0
Control
MuSC cKO
B
M1-like
M2c-like
Tissue res.
M2-like
DC
Vcan
Fn1
Hp
Ifitm6
Chil3
Plac8
Gsr
Nr4a1
Spp1
Fabp5
Gpnmb
Ctsd
Lgals3
Syngr1
Cd36
Cstb
Ctsl
Selenop
Apoe
C1qa
C1qc
Tmem176b
Ms4a7
Tmem176a
Pltp
C1qb
H2–Eb1
Cxcl10
Rsad2
Isg15
Ifit2
Ifit3
Irf7
Ifit1
Ms4a4c
Ccl12
Cd209a
Klrg1
Mgl2
Cbfa2t3
H2–Ab1
Cd74
H2–Aa
H2–DMb1
−1
0
1
2
Expression
D
Macrophages
MuSC cKO vs control
NS
p−value
p-value and log2FC
60
40
20
0
−Log10 P
Ccdc88a
S100a8
Rgs1
Ccl12
Ccl7
Rsad2
Spp1
Ccl2
−0.5
0.0
0.5
1.0
Log2 fold change
total = 2177 variables

**Figure 3.5. Macrophage subpopulation analysis reveals shift towards M2-like polarization with MuSC derived Spp1 ablation.**

(A) Proportion of each macrophage subpopulation by genotype.

(B) Heatmap of top 10 cluster markers for each macrophage subpopulation.

(C) Ratio of M2:M1 macrophage populations by genotype.

(D) Volcano plot of differentially expressed genes where $log_2$fold change < 0.5 and p-value in <0.01.

A

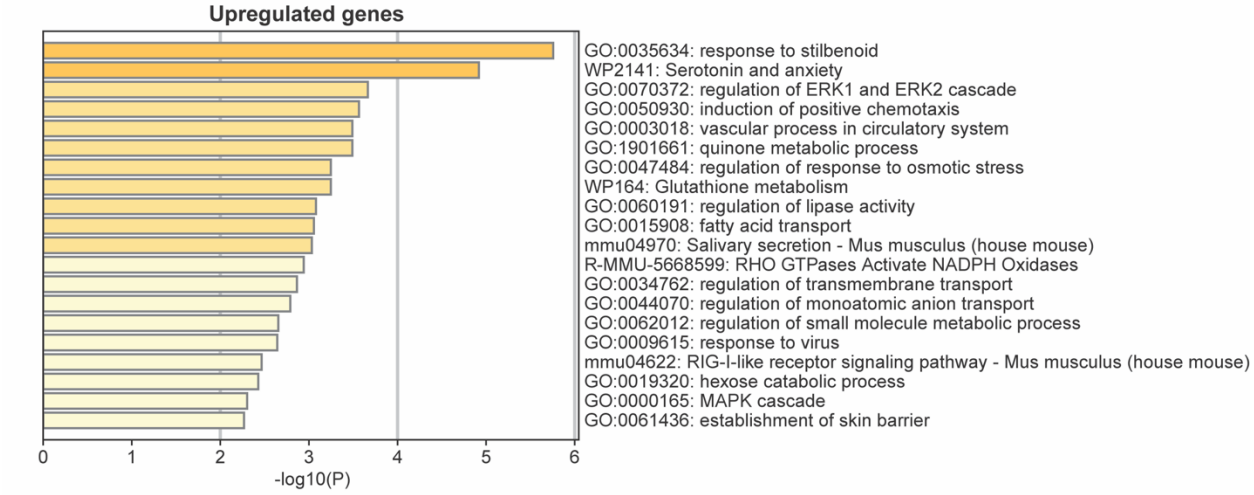
Upregulated genes
GO:0035634: response to stilbenoid
WP2141: Serotonin and anxiety
GO:0070372: regulation of ERK1 and ERK2 cascade
GO:0050930: induction of positive chemotaxis
GO:0003018: vascular process in circulatory system
GO:1901661: quinone metabolic process
GO:0047484: regulation of response to osmotic stress
WP164: Glutathione metabolism
GO:0060191: regulation of lipase activity
GO:0015908: fatty acid transport
mmu04970: Salivary secretion - Mus musculus (house mouse)
R-MMU-5668599: RHO GTPases Activate NADPH Oxidases
GO:0034762: regulation of transmembrane transport
GO:0044070: regulation of monoatomic anion transport
GO:0062012: regulation of small molecule metabolic process
GO:0009615: response to virus
mmu04622: RIG-I-like receptor signaling pathway - Mus musculus (house mouse)
GO:0019320: hexose catabolic process
GO:0000165: MAPK cascade
GO:0061436: establishment of skin barrier
0
1
2
3
4
5
6
-log10(P)

B

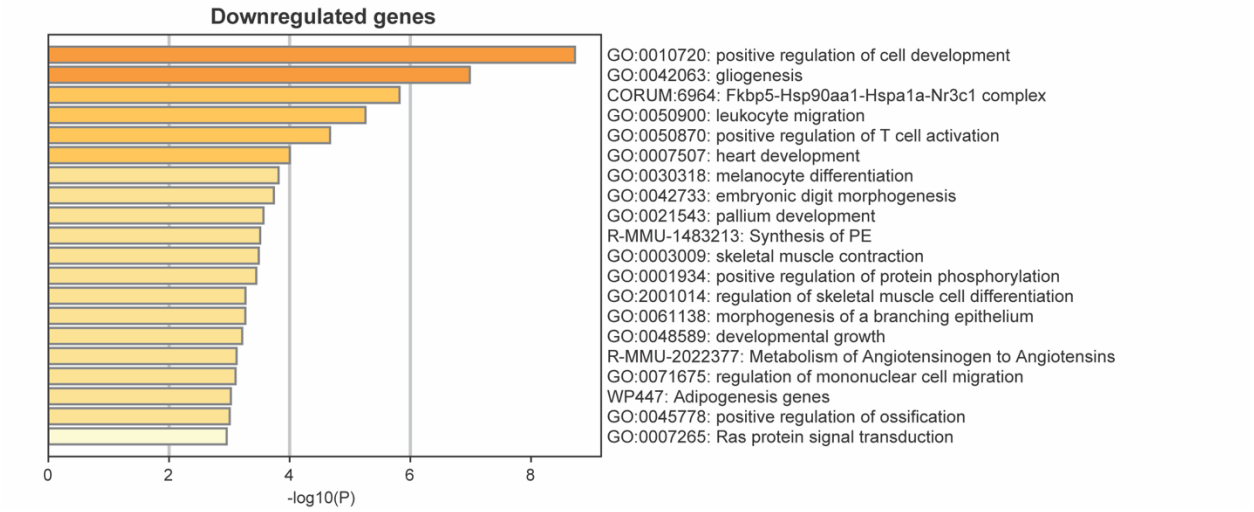
Downregulated genes
GO:0010720: positive regulation of cell development
GO:0042063: gliogenesis
CORUM:6964: Fkbp5-Hsp90aa1-Hspa1a-Nr3c1 complex
GO:0050900: leukocyte migration
GO:0050870: positive regulation of T cell activation
GO:0007507: heart development
GO:0030318: melanocyte differentiation
GO:0042733: embryonic digit morphogenesis
GO:0021543: pallium development
R-MMU-1483213: Synthesis of PE
GO:0003009: skeletal muscle contraction
GO:0001934: positive regulation of protein phosphorylation
GO:2001014: regulation of skeletal muscle cell differentiation
GO:0061138: morphogenesis of a branching epithelium
GO:0048589: developmental growth
R-MMU-2022377: Metabolism of Angiotensinogen to Angiotensins
GO:0071675: regulation of mononuclear cell migration
WP447: Adipogenesis genes
GO:0045778: positive regulation of ossification
GO:0007265: Ras protein signal transduction
0
2
4
6
8
-log10(P)

**Supplemental Figure 3.1. Metascape analysis of FACS isolated ECs from MuSC cKO and control mice.**

(A) Pathways enriched in significantly upregulated DEGs list ($p \leq 0.05$) from MuSC cKO (n=2) and control (n=2).

(B) Pathways enriched in significantly downregulated DEGs list ($p \leq 0.05$) from MuSC cKO (n=2) and control (n=2).

# CHAPTER 4 – CONCLUSIONS

SPP1 is a critically important factor in acute injury of healthy muscle that promotes the necessary immunoreactivity needed to induce rapid muscle regeneration to replace damaged fibers[82]. However, the chronic presence and overexpression of SPP1 such as in the case of DMD creates a reprogrammed muscle microenvironment that is associated with aberrant inflammation, pathological fibrosis, ectopic fat infiltration, failed regeneration and overall more disease severity[18,34]. While the field has understood for the last two decades that the balance of SPP1 is important following injury, the exact mechanism of how the muscle strikes this balance has remained a mystery. The veil that has continued to loom over the field is due to the complexity of SPP1 biology itself. Its seemingly ubiquitous expression in cells within the muscle from myofibers to interstitial cells, how extensively it is post-translationally modified and the number of receptors it binds to has made unraveling how cell-specific sources of SPP1 immensely difficult.

In these studies, we utilized the revolutionary technology of single cell RNA sequencing to begin to elucidate the web of cell-cell communication pathways that are impacted by specific sources of SPP1. We showed that macrophage-derived and muscle stem cell-derived SPP1 play different roles in dystrophic muscle.

In **Chapter 2,** we clarified that macrophage SPP1 regulates macrophage-derived TGFβ1, which has long been hypothesized, but has not been studied in a cell-specific manner until now. scRNAseq allowed us to unbiasedly survey the muscle cellular milleu, which led us to identifying and characterizing two novel stromal cell populations that are enriched in our adipogenesis genes and that we hypothesize give rise to intramuscular fat accumulation. Our data provides a link between macrophage-derived SPP1 and fat accumulation in the muscle via TGFβ regulation of these adipogenically primed stromal cell subtypes.

In **Chapter 3**, we show that MuSC-specific SPP1 regulates the intrinsic MuSC state and plays an inhibitory role of stemness/quiescence and promotes a fibrotic and inflammatory profile. We provide evidence that MuSC SPP1 has a paracrine role in regulating endothelial cell phenotype acting as an inhibitor of angiogenic anti-inflammatory markers, which is an important finding as MuSCs have been shown to be intimately associated with ECs. Additionally, we provide evidence that the improved EC phenotype with loss of MuSC SPP1 may impact macrophage polarization towards an M2c-like state. Our scRNAseq allowed us to determine a MuSC-EC-macrophage regulatory axis via SPP1.

Overall, these studies illustrate that local, cell-specific sources of SPP1 all play unique roles in DMD.

REFERENCES


1. Guiraud S, Aartsma-Rus A, Vieira NM, Davies KE, van Ommen GJB, Kunkel LM. The Pathogenesis and Therapy of Muscular Dystrophies. *Annu Rev Genomics Hum Genet*. 2015;16:281-308. doi:10.1146/annurev-genom-090314-025003

2. Verhaart IEC, Aartsma-Rus A. Therapeutic developments for Duchenne muscular dystrophy. *Nat Rev Neurol*. 2019;15(7):373-386. doi:10.1038/s41582-019-0203-3

3. Batchelor CL, Winder SJ. Sparks, signals and shock absorbers: how dystrophin loss causes muscular dystrophy. *Trends Cell Biol*. 2006;16(4):198-205. doi:10.1016/j.tcb.2006.02.001

4. Moens P, Baatsen PH, Maréchal G. Increased susceptibility of EDL muscles from mdx mice to damage induced by contractions with stretch. *J Muscle Res Cell Motil*. 1993;14(4):446-451. doi:10.1007/BF00121296

5. Blau HM, Webster C, Pavlath GK. Defective myoblasts identified in Duchenne muscular dystrophy. *Proc Natl Acad Sci U S A*. 1983;80(15):4856-4860. doi:10.1073/pnas.80.15.4856

6. Heslop L, Morgan JE, Partridge TA. Evidence for a myogenic stem cell that is exhausted in dystrophic muscle. *J Cell Sci*. 2000;113 ( Pt 12):2299-2308. doi:10.1242/jcs.113.12.2299

7. Dumont NA, Wang YX, von Maltzahn J, et al. Dystrophin expression in muscle stem cells regulates their polarity and asymmetric division. *Nat Med*. 2015;21(12):1455-1463. doi:10.1038/nm.3990

8. Gloss D, Moxley RT 3rd, Ashwal S, Oskoui M. Practice guideline update summary: Corticosteroid treatment of Duchenne muscular dystrophy: Report of the Guideline Development Subcommittee of the American Academy of Neurology. *Neurology*. 2016;86(5):465-472. doi:10.1212/WNL.0000000000002337

9. Quattrocelli M, Salamone IM, Page PG, Warner JL, Demonbreun AR, McNally EM. Intermittent Glucocorticoid Dosing Improves Muscle Repair and Function in Mice with Limb-Girdle Muscular Dystrophy. *Am J Pathol*. 2017;187(11):2520-2535. doi:10.1016/j.ajpath.2017.07.017

10. Wehling-Henricks M, Lee JJ, Tidball JG. Prednisolone decreases cellular adhesion molecules required for inflammatory cell infiltration in dystrophin-deficient skeletal muscle. *Neuromuscul Disord*. 2004;14(8-9):483-490. doi:10.1016/j.nmd.2004.04.008

11. Quattrocelli M, Barefield DY, Warner JL, et al. Intermittent glucocorticoid steroid dosing enhances muscle repair without eliciting muscle atrophy. *J Clin Invest*. 2017;127(6):2418-2432. doi:10.1172/JCI91445

12. Angelini C, Pegoraro E, Turella E, Intino MT, Pini A, Costa C. Deflazacort in Duchenne dystrophy: study of long-term effect. *Muscle Nerve*. 1994;17(4):386-391. doi:10.1002/mus.880170405

13. Hoy SM. Delandistrogene Moxeparvovec: First Approval. *Drugs*. Published online August 11, 2023. doi:10.1007/s40265-023-01929-x

14. Sarepta Therapeutics Announces FDA Approval of ELEVIDYS, the First Gene Therapy to Treat Duchenne Muscular Dystrophy. Sarepta Therapeutics, Inc. Accessed August 18, 2023. https://investorrelations.sarepta.com/news-releases/news-release-details/sarepta-therapeutics-announces-fda-approval-elevidys-first-gene

15. Lok ZSY, Lyle AN. Osteopontin in Vascular Disease. *Arterioscler Thromb Vasc Biol*. 2019;39(4):613-622. doi:10.1161/ATVBAHA.118.311577

16. Franzén A, Heinegård D. Isolation and characterization of two sialoproteins present only in bone calcified matrix. *Biochem J*. 1985;232(3):715-724. doi:10.1042/bj2320715

17. Icer MA, Gezmen-Karadag M. The multiple functions and mechanisms of osteopontin. *Clin Biochem*. 2018;59:17-24. doi:10.1016/j.clinbiochem.2018.07.003

18. Vetrone SA, Montecino-Rodriguez E, Kudryashova E, et al. Osteopontin promotes fibrosis in dystrophic mouse muscle by modulating immune cell subsets and intramuscular TGF-beta. *J Clin Invest*. 2009;119(6):1583-1594. doi:10.1172/JCI37662

19. Kramerova I, Kumagai-Cresse C, Ermolova N, et al. Spp1 (osteopontin) promotes TGFβ processing in fibroblasts of dystrophin-deficient muscles through matrix metalloproteinases. *Hum Mol Genet*. 2019;28(20):3431-3442. doi:10.1093/hmg/ddz181

20. O'Regan A, Berman JS. Osteopontin: a key cytokine in cell-mediated and granulomatous inflammation. *Int J Exp Pathol*. 2000;81(6):373-390. doi:10.1046/j.1365-2613.2000.00163.x

21. Lund SA, Giachelli CM, Scatena M. The role of osteopontin in inflammatory processes. *J Cell Commun Signal*. 2009;3(3-4):311-322. doi:10.1007/s12079-009-0068-0

22. Weber GF, Ashkar S, Glimcher MJ, Cantor H. Receptor-ligand interaction between CD44 and osteopontin (Eta-1). *Science*. 1996;271(5248):509-512. doi:10.1126/science.271.5248.509

23. Chabas D, Baranzini SE, Mitchell D, et al. The influence of the proinflammatory cytokine, osteopontin, on autoimmune demyelinating disease. *Science*. 2001;294(5547):1731-1735. doi:10.1126/science.1062960

24. Steinman L. A molecular trio in relapse and remission in multiple sclerosis. *Nat Rev Immunol*. 2009;9(6):440-447. doi:10.1038/nri2548

25. Agnholt J, Kelsen J, Schack L, Hvas CL, Dahlerup JF, Sørensen ES. Osteopontin, a protein with cytokine-like properties, is associated with inflammation in Crohn's disease. *Scand J Immunol*. 2007;65(5):453-460. doi:10.1111/j.1365-3083.2007.01908.x

26. Sato T, Nakai T, Tamura N, et al. Osteopontin/Eta-1 upregulated in Crohn's disease regulates the Th1 immune response. *Gut*. 2005;54(9):1254-1262. doi:10.1136/gut.2004.048298

27. Zhang F, Luo W, Li Y, Gao S, Lei G. Role of osteopontin in rheumatoid arthritis. *Rheumatol Int*. 2015;35(4):589-595. doi:10.1007/s00296-014-3122-z

28. Bjerre M, Pedersen SH, Møgelvang R, et al. High osteopontin levels predict long-term outcome after STEMI and primary percutaneous coronary intervention. *Eur J Prev Cardiol*. 2013;20(6):922-929. doi:10.1177/2047487313487083

29. Ikeda T, Shirasawa T, Esaki Y, Yoshiki S, Hirokawa K. Osteopontin mRNA is expressed by smooth muscle-derived foam cells in human atherosclerotic lesions of the aorta. *J Clin Invest*. 1993;92(6):2814-2820. doi:10.1172/JCI116901

30. Stępień E, Wypasek E, Stopyra K, Konieczyńska M, Przybyło M, Pasowicz M. Increased levels of bone remodeling biomarkers (osteoprotegerin and osteopontin) in hypertensive individuals. *Clin Biochem*. 2011;44(10-11):826-831. doi:10.1016/j.clinbiochem.2011.04.016

31. Bruemmer D, Collins AR, Noh G, et al. Angiotensin II-accelerated atherosclerosis and aneurysm formation is attenuated in osteopontin-deficient mice. *J Clin Invest*. 2003;112(9):1318-1331. doi:10.1172/JCI18141

32. Piva L, Gavassini BF, Bello L, et al. TGFBR2 but not SPP1 genotype modulates osteopontin expression in Duchenne muscular dystrophy muscle. *J Pathol*. 2012;228(2):251-259. doi:10.1002/path.4026

33. Pegoraro E, Hoffman EP, Piva L, et al. SPP1 genotype is a determinant of disease severity in Duchenne muscular dystrophy. *Neurology*. 2011;76(3):219-226. doi:10.1212/WNL.0b013e318207afeb

34. Capote J, Kramerova I, Martinez L, et al. Osteopontin ablation ameliorates muscular dystrophy by shifting macrophages to a pro-regenerative phenotype. *J Cell Biol*. 2016;213(2):275-288. doi:10.1083/jcb.201510086

35. Todorovic V, Rifkin DB. LTBPs, more than just an escort service. *J Cell Biochem*. 2012;113(2):410-418. doi:10.1002/jcb.23385

36. Heydemann A, Ceco E, Lim JE, et al. Latent TGF-β–binding protein 4 modifies muscular dystrophy in mice. *J Clin Invest*. 12 2009;119(12):3703-3712. doi:10.1172/JCI39845

37. Flanigan KM, Ceco E, Lamar KM, et al. LTBP4 genotype predicts age of ambulatory loss in Duchenne muscular dystrophy. *Ann Neurol*. 2013;73(4):481-488. doi:10.1002/ana.23819

38. Arnold L, Henry A, Poron F, et al. Inflammatory monocytes recruited after skeletal muscle injury switch into antiinflammatory macrophages to support myogenesis. *J Exp Med*. 2007;204(5):1057-1069. doi:10.1084/jem.20070075

39. Gallardo FS, Córdova-Casanova A, Brandan E. The linkage between inflammation and fibrosis in muscular dystrophies: The axis autotaxin-lysophosphatidic acid as a new therapeutic target? *J Cell Commun Signal*. 2021;15(3):317-334. doi:10.1007/s12079-021-00610-w

40. Wang X, Zhao W, Ransohoff RM, Zhou L. Infiltrating macrophages are broadly activated at the early stage to support acute skeletal muscle injury repair. *J Neuroimmunol*. 2018;317:55-66. doi:10.1016/j.jneuroim.2018.01.004

41. Natarajan A, Lemos DR, Rossi FMV. Fibro/adipogenic progenitors: A double-edged sword in skeletal muscle regeneration. *Cell Cycle*. 2010;9(11):2045-2046. doi:10.4161/cc.9.11.11854

42. Juban G, Saclier M, Yacoub-Youssef H, et al. AMPK Activation Regulates LTBP4-Dependent TGF-β1 Secretion by Pro-inflammatory Macrophages and Controls Fibrosis in Duchenne Muscular Dystrophy. *Cell Rep*. 2018;25(8):2163-2176.e6. doi:10.1016/j.celrep.2018.10.077

43. Contreras O, Rossi FMV, Theret M. Origins, potency, and heterogeneity of skeletal muscle fibro-adipogenic progenitors-time for new definitions. *Skelet Muscle*. 2021;11(1):16. doi:10.1186/s13395-021-00265-6

44. La Manno G, Soldatov R, Zeisel A, et al. RNA velocity of single cells. *Nature*. 2018;560(7719):494-498. doi:10.1038/s41586-018-0414-6

45. Merrett JE, Bo T, Psaltis PJ, Proud CG. Identification of DNA response elements regulating expression of CCAAT/enhancer-binding protein (C/EBP) β and δ and MAP kinase-interacting kinases during early adipogenesis. *Adipocyte*. 2020;9(1):427-442. doi:10.1080/21623945.2020.1796361

46. Wang T, Yan R, Xu X, et al. Effects of leukemia inhibitory factor receptor on the adipogenic differentiation of human bone marrow mesenchymal stem cells. *Mol Med Rep*. 2019;19(6):4719-4726. doi:10.3892/mmr.2019.10140

47. Berger E, Géloën A. FABP4 Controls Fat Mass Expandability (Adipocyte Size and Number) through Inhibition of CD36/SR-B2 Signalling. *Int J Mol Sci*. 2023;24(2). doi:10.3390/ijms24021032

48. Uezumi A, Fukada SI, Yamamoto N, Takeda S, Tsuchida K. Mesenchymal progenitors distinct from satellite cells contribute to ectopic fat cell formation in skeletal muscle. *Nat Cell Biol*. 2010;12(2):143-152. doi:10.1038/ncb2014

49. Wosczyna MN, Konishi CT, Perez Carbajal EE, et al. Mesenchymal stromal cells are required for regeneration and homeostatic maintenance of skeletal muscle. *Cell Rep*. 2019;27(7):2029-2035.e5. doi:10.1016/j.celrep.2019.04.074

50. Uezumi A, Ikemoto-Uezumi M, Zhou H, et al. Mesenchymal Bmp3b expression maintains skeletal muscle integrity and decreases in age-related sarcopenia. *J Clin Invest*. 2021;131(1). doi:10.1172/JCI139617

51. Contreras O, Cruz-Soca M, Theret M, et al. Cross-talk between TGF-β and PDGFRα signaling pathways regulates the fate of stromal fibro-adipogenic progenitors. *J Cell Sci*. 2019;132(19). doi:10.1242/jcs.232157

52. Kim HK, Laor T, Horn PS, Racadio JM, Wong B, Dardzinski BJ. T2 mapping in Duchenne muscular dystrophy: distribution of disease activity and correlation with clinical assessments. *Radiology*. 2010;255(3):899-908. doi:10.1148/radiol.10091547

53. Kim HK, Merrow AC, Shiraj S, Wong BL, Horn PS, Laor T. Analysis of fatty infiltration and inflammation of the pelvic and thigh muscles in boys with Duchenne muscular dystrophy

(DMD): grading of disease involvement on MR imaging and correlation with clinical assessments. *Pediatr Radiol*. 2013;43(10):1327-1335. doi:10.1007/s00247-013-2696-z

54. Polavarapu K, Manjunath M, Preethish-Kumar V, et al. Muscle MRI in Duchenne muscular dystrophy: Evidence of a distinctive pattern. *Neuromuscul Disord*. 2016;26(11):768-774. doi:10.1016/j.nmd.2016.09.002

55. Quattrocelli M, Capote J, Ohiri JC, et al. Genetic modifiers of muscular dystrophy act on sarcolemmal resealing and recovery from injury. *PLoS Genet*. 2017;13(10):e1007070. doi:10.1371/journal.pgen.1007070

56. Lemos DR, Babaeijandaghi F, Low M, et al. Nilotinib reduces muscle fibrosis in chronic muscle injury by promoting TNF-mediated apoptosis of fibro/adipogenic progenitors. *Nat Med*. 2015;21(7):786-794. doi:10.1038/nm.3869

57. Dumont NA, Bentzinger CF, Sincennes MC, Rudnicki MA. Satellite cells and skeletal muscle regeneration. *Compr Physiol*. 2015;5(3):1027-1059. doi:10.1002/cphy.c140068

58. Kodippili K, Rudnicki MA. Satellite cell contribution to disease pathology in Duchenne muscular dystrophy. *Front Physiol*. 2023;14:1180980. doi:10.3389/fphys.2023.1180980

59. Relaix F, Bencze M, Borok MJ, et al. Perspectives on skeletal muscle stem cells. *Nat Commun*. 2021;12(1):692. doi:10.1038/s41467-020-20760-6

60. Chazaud B, Sonnet C, Lafuste P, et al. Satellite cells attract monocytes and use macrophages as a support to escape apoptosis and enhance muscle growth. *J Cell Biol*. 2003;163(5):1133-1143. doi:10.1083/jcb.200212046

61. Christov C, Chrétien F, Abou-Khalil R, et al. Muscle satellite cells and endothelial cells: close neighbors and privileged partners. *Mol Biol Cell*. 2007;18(4):1397-1409. doi:10.1091/mbc.e06-08-0693

62. Verma M, Asakura Y, Murakonda BSR, et al. Muscle Satellite Cell Cross-Talk with a Vascular Niche Maintains Quiescence via VEGF and Notch Signaling. *Cell Stem Cell*. 2018;23(4):530-543.e9. doi:10.1016/j.stem.2018.09.007

63. Saleh KK, Xi H, Switzler C, et al. Single cell sequencing maps skeletal muscle cellular diversity as disease severity increases in dystrophic mouse models. *iScience*. 2022;25(11):105415. doi:10.1016/j.isci.2022.105415

64. Babazadeh S, Nassiri SM, Siavashi V, Sahlabadi M, Hajinasrollah M, Zamani-Ahmadmahmudi M. Macrophage polarization by MSC-derived CXCL12 determines tumor growth. *Cell Mol Biol Lett*. 2021;26(1):30. doi:10.1186/s11658-021-00273-w

65. Yi D, Liu B, Wang T, et al. Endothelial Autocrine Signaling through CXCL12/CXCR4/FoxM1 Axis Contributes to Severe Pulmonary Arterial Hypertension. *Int J Mol Sci*. 2021;22(6). doi:10.3390/ijms22063182

66. Ricard N, Scott RP, Booth CJ, et al. Endothelial ERK1/2 signaling maintains integrity of the quiescent endothelium. *J Exp Med*. 2019;216(8):1874-1890. doi:10.1084/jem.20182151

67. Hirata A, Masuda S, Tamura T, et al. Expression profiling of cytokines and related genes in regenerating skeletal muscle after cardiotoxin injection: a role for osteopontin. *Am J Pathol*. 2003;163(1):203-215. doi:10.1016/S0002-9440(10)63644-9

68. Pereira RO, Carvalho SN, Stumbo AC, et al. Osteopontin expression in coculture of differentiating rat fetal skeletal fibroblasts and myoblasts. *In Vitro Cell Dev Biol Anim*. 2006;42(1-2):4-7. doi:10.1007/s11626-006-0003-0

69. Uaesoontrachoon K, Yoo HJ, Tudor EM, Pike RN, Mackie EJ, Pagel CN. Osteopontin and skeletal muscle myoblasts: association with muscle regeneration and regulation of myoblast function in vitro. *Int J Biochem Cell Biol*. 2008;40(10):2303-2314. doi:10.1016/j.biocel.2008.03.020

70. Dumont NA, Wang YX, Rudnicki MA. Intrinsic and extrinsic mechanisms regulating satellite cell function. *Development*. 2015;142(9):1572-1581. doi:10.1242/dev.114223

71. Gioftsidi S, Relaix F, Mourikis P. The Notch signaling network in muscle stem cells during development, homeostasis, and disease. *Skelet Muscle*. 2022;12(1):9. doi:10.1186/s13395-022-00293-w

72. Wen Y, Bi P, Liu W, Asakura A, Keller C, Kuang S. Constitutive Notch activation upregulates Pax7 and promotes the self-renewal of skeletal muscle satellite cells. *Mol Cell Biol*. 2012;32(12):2300-2311. doi:10.1128/MCB.06753-11

73. Shea KL, Xiang W, LaPorta VS, et al. Sprouty1 regulates reversible quiescence of a self-renewing adult muscle stem cell pool during regeneration. *Cell Stem Cell*. 2010;6(2):117-129. doi:10.1016/j.stem.2009.12.015

74. Eliazer S, Muncie JM, Christensen J, et al. Wnt4 from the Niche Controls the Mechano-Properties and Quiescent State of Muscle Stem Cells. *Cell Stem Cell*. 2019;25(5):654-665.e4. doi:10.1016/j.stem.2019.08.007

75. Sacco A, Mourkioti F, Tran R, et al. Short telomeres and stem cell exhaustion model duchenne muscular dystrophy in mdx/mTR mice. *Cell*. 2010;143(7):1059-1071. doi:10.1016/j.cell.2010.11.039

76. Cheng CK, Lin X, Pu Y, et al. SOX4 is a novel phenotypic regulator of endothelial cells in atherosclerosis revealed by single-cell analysis. *J Advert Res*. 2023;43:187-203. doi:10.1016/j.jare.2022.02.017

77. Shimizu-Motohashi Y, Asakura A. Angiogenesis as a novel therapeutic strategy for Duchenne muscular dystrophy through decreased ischemia and increased satellite cells. *Front Physiol*. 2014;5:50. doi:10.3389/fphys.2014.00050

78. Gimbrone MA Jr, García-Cardeña G. Endothelial cell dysfunction and the pathobiology of atherosclerosis. *Circ Res*. 2016;118(4):620-636. doi:10.1161/CIRCRESAHA.115.306301

79. Mack JJ, Mosqueiro TS, Archer BJ, et al. NOTCH1 is a mechanosensor in adult arteries. *Nat Commun*. 2017;8(1):1-19. doi:10.1038/s41467-017-01741-8

80. Bryan MT, Duckles H, Feng S, et al. Mechanoresponsive networks controlling vascular inflammation. *Arterioscler Thromb Vasc Biol*. 2014;34(10):2199-2205. doi:10.1161/ATVBAHA.114.303424

81. Liao JK. Linking endothelial dysfunction with endothelial cell activation. *J Clin Invest*. 2013;123(2):540-541. doi:10.1172/JCI66843

82. Uaesoontrachoon K, Wasgewatte Wijesinghe DK, Mackie EJ, Pagel CN. Osteopontin deficiency delays inflammatory infiltration and the onset of muscle regeneration in a mouse model of muscle injury. *Dis Model Mech*. 2013;6(1):197-205. doi:10.1242/dmm.009993